How do stomata evolve on the road to C_4 photosynthesis?

Yong-Yao Zhao[1,2], Mingju Amy Lyu, FenFen Miao, Genyun Chen, Xin-Guang Zhu[1,2]

1. Center of Excellence for Molecular Plant Sciences, Chinese Academy of Sciences
2. State Key Laboratory for Plant Molecular Genetics

Abstract

Compared with C_3 plants, C_4 plants generally maintain lower stomatal conductance (g_s). C_4 syndrome has been extensively studied in C_4 evolution. Although stomata have long been thought belonging C_4 syndrome, it remains unclear for the stomatal evolution along the path to C_4.

Stomatal pattern was examined in *Flaveria* genus, a C_4 evolutionary model contains species at different evolutionary stages from C_3 to C_4 photosynthesis, which can minimize spurious relationships. Comparative methods, transgenic experiments and semi-*in-vitro* analysis were performed to test molecular basis that underlie anatomic difference.

Novel results: the evolution from C_3 to C_4 species through intermediate species was accompanied by a stepwise rather than abrupt trend in stomatal traits; The initial alteration occurred at Type II and the dramatic change occurred at C_4-like species; The stomata in the evolution of C_4 always evolved towards less and bigger direction; *SD* dominated maximum stomatal conductance (g_{smax}) during the entire C_4 evolutionary process; C_4 evolution selected the reduction of *FSTOMAGEN* expression to decrease g_{smax}.

Our analysis emphasized the stomatal traits in the current C_4 evolutionary model, and provided insights into the manner, mechanism and role of stomata evolving on the road towards C_4.

Key words:

Stomatal traits, *Flaveria*, C_4 evolutionary model, C_4 evolutionary path

The total word count for the main body of the text is 6346. The word count of Introduction, Materials and Methods, Results, Discussion and Acknowledgement is

811, 2293, 2100, 1099 and 43 respectively. This paper includes 8 colour figures. The supporting material includes 18 figures and 5 tables.

Introduction

Compared with C_3 plants, C_4 plants have higher light use efficiency (LUE) as a result of a CO_2 concentrating mechanism (*1*). At the same time, C_4 plants have higher water use efficiency (WUE), could attributed to both lower g_s and higher photosynthetic CO_2 uptake rate (*A*) (*2, 3*). C_4 photosynthesis optimizes water and carbon relations by reducing transpiration without compromising carbon assimilation (*4*). Improvements in water retention capacity enables C_4 plants to better adapt to saline lands, hot and drought environments and open habitats compared with their close C_3 relatives, which raises the possibility that C_4 photosynthesis might have been selected as a water-conserving mechanism (*4*) and that water limitation might be a primary driver of C_4 evolution (*5-7*). The influence of photosynthetic pathway on transpiration cannot be ruled out, the enhancement of water retention capacity may be an adaptation to the C_4 evolution(*3, 8, 9*). Given that C_4 plants have higher potential for biomass productivity, their lower g_s is critical for the survival and fitness of C_4 plants in the field, especially in the world where water shortage is predicted to occur more often.

C_3 plants can reduce transpiration under long-term changed environment by decreasing g_{smax} (*10, 11*), which implies that the decreasing g_{smax} is an option that plants use to reduce water loss. Indeed, phylogenetically informed comparison shows that C_4 plants have lower g_{smax} compared with their close C_3 relatives (*9*), suggesting that the lower g_{smax} contribute to the higher water-conserving ability of C_4 land plants (*3, 9*). C_4 Photosynthesis is a complex trait called C_4 syndrome (*12*). Therefore, low g_{smax}, same as the other features belong to C_4 syndrome, may be a crucial feature for C_4 land plants. However, so far, in comparison with the extensive studies on the other features, relatively little effort has been invested into studying the g_{smax} along the road to C_4 photosynthesis (*13*).

G_{smax} is determined by stomatal density (*SD*) and stomatal size (*SS*). Although

the higher *SD* of C_4 species was observed (*14*), the lower *SD* of C_4 species also exist (*15*). Studies have shown some characteristics previously thought to be different between photosynthetic types have been redeclare to be phylogenetic effects (*16, 17*). Comparative study using plants from different C_4 clades shows that lower g_{smax} in C_4 plants is due to either a smaller stomatal size (*SS*) for some C_4 clades, or lower stomatal density (*SD*) for other clades (*9*), but after accounting for the phylogenetic effects, *SD* in C_4 is lower than C_3 species (*9*). However, the influence of photosynthetic pathway on *SD* or *SS* is at the margin of statistical significance (*9*), implying that there might be disturbance from other factors unrelated to the photosynthetic type. For example, the complicated thing is that the stomatal development is affected by many environmental conditions, such as soil moisture and fertility status (*18-21*). The effects of photosynthetic pathways on stomata may be disturbed by environmental influences. Therefore, the direct evidence is now needed from the more similar C_3 ancestors to C_4 plants to test the stomatal evolution accompanying the C_4 evolution.

Stomatal development is controlled by a well-studied genetic program (*22*), which mainly involves a series of ligands and the transmembrane receptors, leading to downstream changes of mitogen-activated protein kinase (MAPK) and transcription factors (*22*). TOO MANY MOUTHS (TMM) and ERECTA-family (ERfs: ER, ERL1, ERL2) are receptor-like kinases that negatively regulate stomatal development (*23, 24*), and the TMM interacts with ERfs (*23, 25*). The ligands that bind to ERfs and TMM receptors are mainly EPIDERMAL PATTERNING FACTOR/EPIDERMAL PATTERNING FACTOR-LIKE family (EPF/EPFL-family) peptides (*26*). Overexpression of *EPF1* decreases *SD* (*27*). *EPF2* has a similar genetic effect as *EPF1* (*28*). STOMAGEN prevents the phosphorylation of downstream receptors, which results in the changed expression of basic Helix-loop-Helix (bHLH) paralogs, SPCH, MUTE and FAMA, ultimately positively regulates stomatal development (*29-32*).

C_4 plants are considered to have evolved gradually from C_3 ancestors through intermediate forms that have been found in some species (*33, 34*). The intermediate

species with features between C_3 and C_4 have been confirmed as true intermediate phase on the path to C_4 by phylogenetic and biochemical modeling, which in keeping with detailed experimental studies, especially in *Flaveria* genus (*7, 33, 35, 36*). For the purpose, we chose *Flaveria* genus as the model for the studies of C_4 evolution. *Flaveria* genus contains numerous and close species with different photosynthetic type, especially multiple intermediate species which entirely covers the different and sequential stages of C_4 evolution i.e. C_3, C_3-C_4 type I, C_3-C_4 type II, C_4-like and C_4. The large number of intermediate *Flaveria* species, and *Flaveria* is the youngest genus in C_4 evolution (*37*), suggest that it is still undergoing C_4 evolution (*38*). A close relationship between *Flaveria* species can minimize the impact of non-photosynthetic types, usually manifested in their similar morphologies and habitat environment (*39-42*). These make *Flaveria* genus has been the preferred object for the research on evolutionary process from C_3 to C_4 (*33*), and indeed there has been a large number of studies on their physiology, structure, biochemistry and molecule (*36, 38, 43-45*). The current C_4 evolutionary model is largely based on these studies on *Flaveria* species, which made *Flaveria* genus as the chief model system for the understanding of C_4 evolution (*33, 46*). The current C_4 evolution model involves many features *(36, 40, 44, 45, 47-49)*. In short, bundle sheath cells and vein density begin to develop before the appearance of C_4 metabolism (*33, 43, 50*). Glycine decarboxylase (GDC) transfers from mesophyll cells to bundle sheath cells (*51*), therefore, photorespiration acts as a modest CO_2-concentration mechanism (*50*), and promote the formation of C_4 metabolism (*33, 36*). Although stomata have long been thought to be a member of C_4 syndrome and might related to C_4 evolution (*9, 12*), the cognition for it in the C_4 evolution is still limited. Now it is significant to add stomatal traits to the current C_4 evolutionary model to promote our understanding the stomatal evolution along the path to C_4. Therefore, this study aims to answer the following questions: 1) In the context of the current C_4 evolution model, will stomatal traits and g_{smax} change with the innovation of photosynthetic type, how to change and what's the evolution direction? 2) What's the molecular mechanism underlying the change of the g_{smax} during C_4 evolution? 3) What are the role and drivers of g_{smax} in the evolutionary

process towards C_4 photosynthesis?

Result

Maximum stomatal conductance and stomatal pattern during the evolution of C_4 photosynthesis

As a model of C_4 evolution, there are distinct evolutionary phases in *Flaveria* genus (Fig 1a). The maximum value of operational g_s (marked with circles on figure) for C_3 *Flaveria* species under saturated light intensity was higher than that for C_4 species, indicating that the C_3 *Flaveria* species tends to have a higher g_s (Supplementary Fig 1a). The pore length of stomata was approximately equal to 0.41×stomatal length, and the guard cell width was approximately equal to 0.33×stomatal length (Supplementary fig. 19). Through measuring stomatal density and stomatal length, we calculated the g_{smax} for *Flaveria* species. The results show that, whether growing under outdoor natural light or constant light in the greenhouse, the g_{smax} decreased gradually from C_3 through intermediate species to C_4 species (Fig 1b,c,d,e). A significant correlation was found between the g_{smax} and g_s under saturated light for the *Flaveria* species with different photosynthetic types (Fig 1f). Under saturated light, the g_s of *son* (Type I) was extremely high (marked with circle on figure), matching with its highest g_{smax} within the *Flaveria* genus (Fig1d, Supplementary Fig 1a). Similar to that under the saturated light intensity, the WUE (A/g_s) of *rob* (C_3) measured under unsaturated light intensity was higher than that of *bid* (C_4), and the g_s of *rob* was 71% higher than that of *bid* (Supplementary Fig. 1d). The observed reductions in both g_s and g_{smax} of C_4 and C_4-like *Flaveria* species compared to C_3 and Type I species suggest that the decrease in g_{smax} contributes to the decrease in g_s during C_4 evolution.

In comparison to C_4 and C_4-like photosynthesis, the stomatal densities (*SD*) of C_3 and Type I photosynthesis on the abaxial leaf surface of *Flaveria* were nearly 150% higher (Fig. 2a,b,c,d). With the progression from C_3 to C_4 species, there was a distinctly gradual decrease in *SD* (Fig. 2a, c). The difference in *SD* and *SS* between C_3 and Type I species wasn't as large as that between C_3 and C_4 species; and the *SD* and

SS of Type II species fell in between Type I and C_4-like species (Fig. 2b,d). The *SD* of C_4 and C_4-like species were similar, although the *SD* of C_4-like species was slightly less than that of C_4 (Fig. 2b,d). For the adaxial leaf surface, the *SD* of C_3 species was again higher than that of the C_4 species, although the difference between *SD* in the intermediate species was less significant (Supplementary fig. 3a,b,c,d). There was a strong positive correlation of g_{smax} and *SD* either on abaxial leaves (R^2=0.8955, p<0.0001) (Fig. 2e) or on adaxial leaves (R^2=0.9165, p<0.0001) (Supplementary fig. 3e) and a significant negative correlation of g_{smax} and *l* on abaxial leaves (R^2=0.2596, *p*<0.005) (Fig. 2f), indicating the *SD* determined the change of g_{smax}, not stomatal size (SS). *SD* and *l* showed a significant negative correlation on abaxial leaves (R^2=0.5093, *p*<0.0001) (Fig. 2g) or on adaxial leaves (R^2=0.2055, *p*<0.05) (Supplementary fig. 3g), the same as reported previously (*10, 52, 53*).

Flaveria species, i.e. *rob, ram* and *bid,* were chosen to represent C_3, intermediate and C_4 species, respectively, to analyse the ratio between stomatal number and the number of epidermal cells, i.e. the stomatal index (*SI*). The *SI* of *rob* was nearly 50% higher than *bid* and *ram* in plants grown in either greenhouse or outdoors, suggesting that the proportion of stomata occupying the epidermis, contributed to the highest *SD* in *rob* (Fig. 2h). In addition to the analysis of *Flaveria* plants grown from cuttings, we also planted *Flaveria* germinated from seeds. Results show that the *SD* of C_3 species was higher than C_4 species, consistent with the results from cuttings (Supplementary Fig. 4).

Comparison of the sequence and transcription abundance of genes related to stomatal pattern between C_3 and C_4 *Flaveria* species

The signaling pathway for stomatal development has been studied extensively (*54*). We identified amino acid sequence encoded by homologs of stomatal development related genes in *Flaveria*. Amino acid sequence alignment analysis showed that epidermal patterning factor/epidermal patterning factor-Like gene family (*EPF*/*EPFL*-family) homologs was conserved at the C-terminal part of amino acid sequence (Fig. 4A, Supplementary fig. 5). Members of *EPF*/*EPFL*-family genes

encode secretory proteins containing signal peptides at the N-terminus and functional domains at the C-terminus (*27, 28, 55*). Analysis shows that the hydrophobicity of EPFs/EPFL homologs in *Flaveria* was similar to EPF/EPFL in Arabidopsis (Supplementary fig 6), implying the homologs are also the secretory proteins and should have the same physiological function as EPF/EPFL. We hypothesized that either the amino acid sequence or the expression of stomatal development related genes changed during C_4 evolution. Analysis results reveals no differences within the functional region of amino acid sequence for STOMAGEN, EPF1 and EPF2 homologs between C_3 and C_4 species (Fig. 5a, Supplementary fig. 5a, b), indicating the change of amino acid sequence is unlikely to be a cause of the changed *SD* in C_4 evolution.

As up-regulation of transcription has been a major approach to increase the expression of many genes participating in the building of C_4 phenotype during C_3 to C_4 evolution in *Flaveria* **(*36, 44*)**, we compared the transcript abundance of stomatal development related genes between C_3 and C_4 *Flaveria* species. The expression patterns of known C_4 related genes in our data analysis were same as the previous works, which indicates that our data collection and analysis procedure were reliable (Supplementary Fig. 11) (*36, 44*). We found that the homologs of most stomatal development related genes showed higher transcript abundance in developing tissues as compared to developed tissues (Fig. 3b), which is consistent with their function of regulating stomatal differentiation in developing leaf (*27, 30, 32, 56*). *STOMAGEN*, *EPF1*, *SDD1* and *TMM* showed obviously lower expression levels in C_4 species than in C_3 species (Fig. 3c). Among these genes, *STOMAGEN* was the one that changed the most (Fig. 3c) and showed the most significant difference (Fig. 3d). *EPF1*, *SDD1* and *TMM* are negative regulators for stomatal development (Supplementary table 3) (*26-28, 57*). Actually SD in C_4 species was lower than that in C_3, indicating these genes are not be the factors responsible for the decrease in *SD* of C_4 species. *STOMAGEN* is a positive regulator of *SD* (Supplementary table 3) (*26, 30, 31*), whose lower expression in C_4 species was consistent with the decreased *SD* in C_4 species (Fig.2a,b,c,d,Supplementary Fig. 3c, d). RT-qPCR quantification of the expression

levels of *STOMAGEN*, *EPF1*, *EPF2* homologs between C_3 and C_4 species grown under our conditions also confirmed the results from RNA-SEQ (Fig. 3e, Supplementary fig. 14). In this study, we renamed *STOMAGEN* in *Flaveria* as *FSTOMAGEN*.

There are considerable differences in amino acid sequence of signal peptide of *STOMAGEN* homologs, especially between species with large evolutionary distance (Fig. 4a). The functional domain of *STOMAGEN* is however conserved, not only between different *Flaveria* species (Fig. 5a), but also between species that have a large evolutionary distance (Fig. 4a). A phylogenic tree constructed for *STOMAGEN* from different plants suggest *STOMAGEN* homologs of species in the genus *Flaveria* are extremely conserved (Supplementary fig. 18). In Arabidopsis, increased expression of *STOMAGEN* increases *SD*; experiments with exogenously applied STOMAGEN peptides shows that the signal peptide is not required for STOMAGEN to induce increased SD (*30, 31, 55, 56*). Previous studies showed that overexpressing rice *STOMAGEN* homologs increases *SD* in Arabidopsis and decreased expression of rice *STOMAGEN* homologs reduces *SD* in rice (*58-60*), implying *STOMAGEN* homologs also regulate stomatal development in other species besides Arabidopsis. When plants are grown under conditions that promote or inhibit stomatal development, the expression of *STOMAGEN* is known to increase or decrease, respectively (*18, 56, 61*). A similar modulation of *STOMAGEN* expression levels was observed for *rob* when grown at different light conditions (Supplementary Fig 9).

To confirm that *FSTOMAGEN* can induce stomatal generation and assess the ability of *FSTOMAGEN* to regulate stomatal development, we overexpressed the *FSTOMAGEN* in *Arabidopsis*. Specifically, we recombined the signal peptide of *STOMAGEN* from *Arabidopsis* to the functional region of *FSTOMAGEN* and named the hybrid gene as AFSTO (Fig, 4e). Overexpressing either the AFSTO or the intact *FSTOMAGEN* (FSTO) from *F.rob* into *Arabidopsis* resulted in similar increased *SD* (Fig. 4f,g,i,j, Supplementary fig 15). Identification of transcription showed successful transgenes and the expression level of the AFSTO or FSTO increased with the increase in SD (Fig. 4f, g, i, j). Furthermore, overexpression of *FSTOMAGEN* also

induced clustered stomata (Fig. 4k, Supplementary fig 20), as also reported earlier for the over-expression of *STOMAGEN* (*30*). To further confirm that *FSTOMAGEN* can increase *SD* in *Flaveria*, we synthesized a peptide representing the FSTOMAGEN functional region, consisting of 45 amino acids. In order to confirm our synthesized peptides that have been folded were biologically active, the FSTOMAGEN peptides were applicated in vitro on the leaves of Arabidopsis and resulted in increased *SD* and cluster stomata (Fig 4b, Supplementary fig 17b). Application of the peptides on the leaves of *bid* also increased *SD* and *SI* and caused stomatal cluster (Fig 4c, d, Supplementary fig 17a). These results demonstrate that, in addition to its *in vivo* function, *in vitro* application of FSTOMAGEN also directly positively regulate *SD* in *Flaveria*. This is consistent with the notion that *STOMAGEN* is expressed in mesophyll cells and secreted out of cells to influence the stomatal development in the epidermal layer in *Arabidopsis* (*30, 31*).

The transcript abundance of *FSTOMAGEN* during C_4 evolution in *Flaveria*

We examined the copy number of *FSTOMAGEN* in *Flaveria* using blastn with the coding sequence of *FSTOMAGEN* as query sequence against the assembled contigs of each *Flaveria* species from 1KP. Results show that there was only one hit sequence with e-value less than 10^{-5} in each species, suggesting that there is a single copy of *FSTOMAGEN* in *Flaveria* (Supplementary fig. 12). Therefore we can ignore the impact of other *FSTOMAGEN* paralogs on stomatal development, and there will be no quantitative errors in the gene expression levels caused by other paralogs that were not considered. Examination of the RNA-seq data of *Flaveria* showed that the expression levels of *FSTOMAGEN* in C_3 species were markedly higher than those in C_4 species along different developmental stages of leaves (Fig. 5c). During leaf growth and development, the expression of *FSTOMAGEN* in both *bid* and *rob* increased first, reaching the highest level at leaf development stage 3 (leaf length 1.5 cm) or 4 (leaf length 2.0 cm), and then declined (Fig. 5c). The similar patterns of *FSTOMAGEN* expression in these two *Flaveria* species indicates that it would be valid to compare the *FSTOMAGEN* expression levels in leaves at the same

development stage between *Flaveria* species. The expression level of *FSTOMAGEN* in *bid* (C_4) was lower than that in *rob* (C_3), and that of *ram* (intermediate) lied between them (Fig. 5b). This encouraged us to test more *Flaveria* species with different photosynthetic types. Similar results were obtained with either RNA-seq or RT-qPCR (Fig. 5d, Supplementary Fig. 13), where we found the gradual decrease of *FSTOMAGEN* expression from C_3 to intermediate species to C_4 species. Together these results suggest that the gradual change in the *FSTOMAGEN* expression levels between different species underlay the stepwise change in *SD* along C_4 evolution.

The expression of *FSTOMAGEN* homologs for species with different photosynthetic type in multiple C_4 lineages.

To gain insight into whether *STOMAGEN* homolog might be a generic factor leading to the difference in *SD* between C_3 and C_4 species in higher plants, we tested its expression level in different C_4 lineages other than the *Flaveria genus*. The *SD* of abaxial leaf in C_3 rice was 240% higher than that in C_4 maize, consistent with a 574% higher g_s in rice compared to maize (Fig. 6a, c). The stomatal length (l) in maize was 133% longer (Fig. 6b). We analysed the transcript abundance of *STOMAGEN* homologs, since there are two and three paralogs of *STOMAGEN* in rice and maize respectively (*58*), only one in rice and two in maize are expressed. The *STOMAGEN* homologs in rice had much higher transcript abundance than those in maize (Fig. 6f), while the transcript abundance of other stomatal development related genes did not differ to the same extent between rice and maize (Fig. 6e). This result encouraged us to test more C_4 lineages (Fig. 6g). C_4 photosynthesis related genes were indeed higher in C_4 species, suggesting the data and analysis pipeline can be used to compare the differences in expression of genes between C_3 and C_4 photosynthetic types (Fig 6h). It was showed that the expression levels of *STOMAGEN* homologs for C_4 were lower than those for C_3, while intermediate had expression between them (Fig 6i).

Method

Plant materials, sample condition and data sources

All *Flaveria* species used in this study were kindly provided by Prof. Rowan F. Sage (University of Toronto). Plants used for stomatal phenotyping were re-grown from cuttings. Placed in an environment humidified with humidifiers to generate roots. After plants generated roots, they were transferred outdoors (Institute of Plant Physiology and Ecology, Chinese Academy of Sciences, Shanghai, China), and transplanted into 4-L pots filled with topsoil in April. In July, the number of stomata on abaxial and adaxial surfaces of leaves were counted. Another batch of *Flaveria*, which were also grown from cuttings, were transferred to the phytotron (Center of Excellence for Molecular Plant Sciences, Chinese Academy of Sciences, Shanghai, China). Growth temperature of the phytotron was maintained at 25-28□, photoperiod was maintained at 16h light / 8h dark, relative humidity (RH) was at 60-65% and photosynthetic photon flux density (PPFD) was maintained at about 180 μmol m^{-2} s^{-1}. Two months later, the numbers of stomata on the abaxial and adaxial surfaces of leaves were counted. RNA was extracted from 1.5~3.0 cm long young leaves on the axial shoot which were still expanding. Three hours before sampling, we provided sufficient water to ensure that plants were not water limited, since drought and water status can affect expression levels of *STOMAGEN* and *SD* (*18*, *20*). Gene expression was also examined under normal growth conditions by RT-qPCR for the *rob*, *ram* and *bid*, which are representative of C_3, intermediate and C_4 species in the *Flaveria* genus. These three species were grown in the same phytotron with the same environmental conditions, except that we did not water plants before sampling. To test whether plants grown from cuttings or from seeds show difference in the *SD*, we further grew *Flaveria* species from seeds in phytotron and examined stomatal properties. Same environmental conditions were maintained for phytotron as above. Two months after the germination of seeds, we counted stomatal number.

All plants were well watered to avoid drought stress during their growth. We supplied the same amount of commercial nutrient solution (Peters Professional, SCOTTS, N:P:K = 20:20:20+TE, at recommended dose for application) to the different species to avoid nutrient deficiency.

Rice (*Oryza Sativa Nipponbare*) and maize (*Zea maize* B73) were grown in the greenhouse (Center of Excellence for Molecular Plant Sciences, Chinese Academy of Sciences, Shanghai, China) under a PPFD of 550 umol/m^2/sec, a photoperiod of 12h light / 12h dark, and a daytime temperature of around 31℃ and a night-time temperature of around 22℃. The Relative humidity was maintained at around 50-55%. The plants were regularly watered to avoid drought stress.

In addition to the expression data collected by in this study, we also used public data for comparison of transcript abundance. Considering that stomatal development related genes are mainly expressed in young tissues, in each of these used public data source, samples for young leaves were included. For the *Flaveria*, the samples data from four source containing the leaves of plants grown under normal condition were analysed. The first data source is the One Thousand Plants (1KP) Consortium, and we subsequently analyzed the data according to the methods described in previous work (*62, 63*); The second and third data sources were Mallman et al (2014) (*36*) and Udo Gowik et al (*44*); The fourth data source was Kumari Billakurthi et al (2018) (*64*). The last three data sources are all from Heinrich-Heine-University. For the second and third data source, the second and fourth visible leaves were sampled; the second leaf was not completely mature, and stomatal developmental related genes were still actively expressed. In addition to *Flaveria*, transcripts of C_3 and C_4 species from other C_4 lineage sequenced from 1KP were assembled using Trinity (*65*) with default parameters. Transcript abundances were analyzed by mapping the reads to assembled contigs for corresponding samples using the RSEM package with mapping option of bowtie 1 (*66*), and outliers that less than Q1 (lower quartile) - 1.5IQR (interquartile range) and greater than Q3 (upper quartile) + 1.5IQR (interquartile range) were removed. Expression levels for stomatal development related genes in developing leaves for rice and maize were obtained from Wang et al. (*67*).

Conservation and hydrophobicity analysis of proteins

Amino acid sequence of the homologs of *STOMAGEN*, *EPF1* and *EPF2* were

aligned by clustalx, and graphs for the multiple alignments were drawn with ESPrit 3.0 (*68*) (http://espript.ibcp.fr/ESPript/cgi-bin/ESPript.cgi). Hydrophobicity of proteins was determined by ProtScale (*69*) (https://web.expasy.org/protscale/).

Construction of the phylogenetic tree of *STOMAGEN*

In order to construct the gene evolutionary tree of *STOMAGEN*, we searched the orthologs of *STOMAGEN* in 28 representative species among Viridisplantae as demonstrated in (*70*),The protein sequences of representative species were downloaded from Phytozome (https://phytozome.jgi.doe.gov/). Orthologs of STOMAGEN were predicted applying OrthoFinder (V 0.7.1) (*71*)using default parameters. Proteins sequences of STOMAGEN orthologs were then aligned using MUSCLE (*72*). We than inferred the gene phylogeny using both maximum likelihood (ML) and Bayesian-inference (BI) methods. The ML tree was constructed applying RAxML (V2.2.3) (*73*), where bootstrap scores were obtained by running 100,000 independent trees. BI tree was built applying MrBayes package (v 3.2.1) (*74*), where posterior probabilities were calculated by running 2000,000 generations with the first 2000 generations being used as burn-in. In both cases, PROTGAMMAILG model (General Time Reversible amino acid substitution model with assumption that variations in sites follow gamma distribution) was used to infer the gene phylogeny. The protein sequence of AT4G14723 (*CLL2*) from A. thaliana was used as outgroup as it showed the highest identity with STOMAGEN in A. thaliana, with a protein identity of 26.97% and E-value of 0.037 based on Blastp (*75*). Protein sequences for the *Flaveria* species were predicted using OrfPredictor (*76*) based on de novo assembled transcripts as described in (*77*).

Measurement of stomatal conductance (g_s)

The LI-6400 Portable Photosynthesis System (Li-Cor, Inc., Lincoln, NE, USA) was used to measure g_s on the youngest fully expanded leaves from approximately three-months-old *Flaveria* plants. The cuvette temperature was maintained at 25□, the PPFD was at ~500 μmol/m²s and the CO_2 concentration was at around 400 ppm.

Chamber humidity was matched to ambient air humidity. Leaf-to-air vapor pressure difference (VPD) was maintained around 1.1 kPa. Before the g_s measurements, *Flaveria* plants were maintained under constant light with a PPFD of ~500 μmol/m^{2}s until g_s reached a steady state. External environments during the g_s measurements for rice and maize were controlled to be their growth conditions. In maize and rice, the16-day-old third leaves which were the youngest mature leaves, were used for gas exchange measurements (*67*).

Phenotyping stomatal traits and the calculation of g_{smax}

The youngest fully expanded leaves (usually the third or fourth leaves from the apex in *Flaveria*) at the main stem were used to phenotype stomata related traits. In *Flaveria* and maize, stomata related traits were observed using both nail polish method and epidermis directly peeled from leaves (*6*, *53*). For the first method, nail polish was painted on both leaf surfaces to produce the impressions of epidermis. After drying of the nail polish, the nail polish was peeled off the leaf and placed on a microscope slide for examination. For the second method, leaf epidermis was peeled off manually and transferred onto microscope slide. For the count of SD in Arabidopsis, the rosette leaves was soaked in 9:1 (V/V) ethanol:acetic acid overnight, washed with water and cleared in chloral hydrate solution (glycerol:chloral hydrate:water, 1:8:1) overnight, and then stomata of Arabidopsis were stained with Safranin-O, finally leaves were placed on a microscope slide for imaging. Light microscope (smarte; CNOPTEC), camera and image processed software (OPTPRO; CNOPTEC) were used to observe and image epidermis at 100x magnification in *Flaveria*. Center of a leaf was chosen to count stomatal density and measure stomatal length. Five stomata randomly chosen along a diagonal of the varnish peels or epidermis were measured for stomatal length.

G_{smax} was calculated using the follow equation (*52*):

$$g_{smax} = \frac{d}{v} \cdot \mathrm{D} \cdot a_{max} / (e + \frac{\pi\sqrt{a_{max}/\pi}}{2})$$

The constants d is the diffusivity of H_2O in air; the constant v is the molar volume of air; D is the stomatal density; a_{max} is the maximum stomatal pore area which is calculated as $a_{max} = \pi p^2/4$ in *Flaveria* species, and the p is the stomatal pore length; e is the stomatal pore depth, which is known as equal to guard cell width.

RNA isolation, semiquantitative RT-PCR and quantitative real-time PCR

The young leaf samples taken from the main stem in *Flaveria* or the developing rosette leaves in Arabidopsis were immediately frozen in liquid nitrogen and used directly for RNA extraction. Total RNA was extract from the young leaves using the PureLink RNA Mini kit (Thermo Fisher Scientifc). The first-strand cDNA was synthesized by the TransScript One-step gDNA Removal and cDNA Synthesis SuperMix (TRANSGEN). Semiquantitative RT-PCR was performed with Phanta® Max Super-Fidelity DNA Polymerase (vazyme). The actin8 was chosen as the loading control. Real-time PCR was performed on the CFX connect™ (Bio-Rad) with the UNICON™ qPCR SYBR ®Green Master Mix (YEASEN) according to the manufacturer's instructions. The calculation of expression according to the $2^{-\Delta\Delta CT}$.

The expression stability of internal reference genes for the quantitative real-time PCR was assessed by the software: geNORM and NormFinder (*78*, *79*). Specifically, we first calculated the coefficient of variations (CV) of all genes in different *Flaveria* species. After that, all genes were sorted according to the calculated CV values. 150 genes with the lowest CV were selected as potential candidate reference genes. Among these, those with mean expression level >300 were chosen as candidate reference genes. We also included those commonly used house-keeping genes, which include *UBC9* (AT4G27960), *UBQ11* (AT4G05050), *ACT7* (AT5G09810), *GAPDH* (AT1G13440), *EF1a* (AT5G60390), *CACMS* (AT5G46630) (Supplementary fig. 6a, b, d), as the internal reference genes in this study. The specificity of the primers (Supplementary table 2) for all these candidate reference genes were identified by agarose electrophoresis (Supplementary fig. 6c). With Genorm (Supplementary fig. 6e) and Normfinder (Supplementary fig. 6f), we concluded that *ACT7*, *EF1a* and *HEME2* showed stable expression levels across *rob*, *ram* and *bid*. *EF1a* and *ACT7* are classic reference genes, and they showed minor variations under different conditions. The

geometrical means of the expression level of *ACT7* and *EF1a* were finally used as normalization factors. All primers used for RT-qPCR are listed in Supplementary table 2. For each gene, three technical replicates and at least three biological replicates were performed.

Vector construction and transformation

A list of primer sequences were used for plasmid construction (Supplementary table 2). The *STOMAGEN* and *FSTOMAGEN* DNA sequences, named ATSTO-cDNA and FloSTO-cDNA respectively, were PCR-amplified from cDNA in Arabidopsis and *rob*. To obtain the AFSTO fragment, the signal peptide region of *STOMAGEN* was cloned from ATSTO-cDNA by PCR-amplification, and the functional region of *FSTOMAGEN* was PCR-amplified from FloSTO-cDNA. The signal peptide and functional region were combined by fusion PCR. To obtain an intact *FSTOMAGEN* (FSTO) gene, the whole gene in *rob*, including the signal peptide, propeptide and the *STOMAGEN* functional region, was amplified from the cDNA of *rob*. To over-express AFSTO and FSTO, the AFSTO and FSTO were cloned separately to a pcambia-3300 binary vector which has a CaMV 35S promoter. This construct was introduced into *A. tumefaciens* strain GV3101, transformed into Arabidopsis using a floral dipping procedure. Transgenic lines were selected on soil that had been treated with a diluted solution of phosphinothricin (diluted 3000 times) over night. About a month after the seeds were sowed on the soil, the stomata were observed on the biggest mature rosette leaf. The phenotype of Arabidopsis T1 and T2 generations was observed at the 400x magnification using the light microscope. For each epidermal peel, five fields were counted for density.

Refolding of synthetic *FSTOMAGEN*

Chemically synthesized peptide (Synthesized peptide sequence: IGSVKPTCTY NECRGCRSRCRAEQVPVEGNDPINSAYHYRCICHR, Sangon Biotech, Shanghai, China) was dissolved in 20 mM Tris-HCl, pH 8.8, and 50 mM NaCl and then dialysed (Sangon Biotech,0.5 KD-1 KD) for 1 day at 4□ against 0.5 mM glutathione (reduced

and oxidized forms, Macklin) and 200 mML-arginine (meilunbio) at pH 8.0, which were further dialysed three times against 20 mM Tris-HCl, pH 8.8, and 50 mM NaCl for 1.5 days to remove glutathione.

Stomata induction assay

When the first true leaf or cotyledons appeared in *bid* and Arabidopsis that had germinated in 1/2 MS sterilized solid medium, F*STOMAGEN* peptide was applied on the plants. After the *bid* and Arabidopsis was further incubated in 1/2 MS liquid medium at 22℃ for 5 days, stomatal number on the abaxial surfaces for the first true leaf and cotyledons was counted under a differential interference contrast microscope (DIC)**.**

Plotting and statistical analysis

The correlation, linear regressions and t-test (a=0.05) was performed by GraphPad Prism 8. Differences between means of multi-groups were assessed with one-way analysis of variance (ANOVA). Duncan's multiple range test was performed using the agricolae package of the R (https://www.r-project.org/) to detect differences between two groups. The A and g_s at the saturated light intensity were digitized from figure 1 and figure 3 in (*2, 80*) using the OriginPro 2018.

Accession numbers

The *Flaveria* read data have been submitted to the National Center for Biotechnology Information Short Read Archive under accession numbers: SRP036880, SRP036881, SRP036883, SRP036884, SRP036885, SRP037526, SRP037527, SRP037528, SRP037529, SRP006166, SRP169568. The *Flaveria* RNA-Seq datasets from 1KP Consortium were available at National Center for Biotechnology Information (NCBI) Gene Expression Omnibus (GEO) under accession number: GSE54339. The rice and maize RNA-seq datasets under accession number: GSE54274.

Discussion

Many recent works have shown that transpiration requirements may play an important role in the evolution of C_4 photosynthesis (*3, 4, 9*). The short-term regulation of the gas exchange capacity of stomata is mainly the dynamic opening and closing(*81*). But on an evolutionary scale, the central to adapting to the gas exchange demand for a long-term should be the adjustment of g_{smax} i.e. stomatal density and stomatal size (*9-11, 52*), may be due to the higher energy cost of metabolism required for stomatal opening and closing. In fact, we found that the g_{smax} in *Flaveria* is significantly correlated with the measured operating g_s (supplementary fig 1). In order to study the stomatal evolution accompanying the innovation of photosynthetic pathway, we chose the genus *Flaveria*. The genus *Flaveria* (Asteraceae) has been widely used as a model system for studying the ecophysiological and molecular biology of the C_4 evolution, and it includes the species with different photosynthetic type and very close evolutionary distance. C_3 photosynthesis in the genus is undoubtedly a condition of ancestors, and each level of photosynthetic type is the ancestral condition of the next level. *Flaveria* represents an C_4 evolutionary model that minimizes differences in habitat. *Flaveria* species occur in similar habitats in Mexico and the southern USA(*39, 40*), exhibit similar morphologies and are frequently found in disturbed conditions on alkaline or gypseous soils (*39, 42*). Both C_3 and C_4 species of *Flaveria* thrive in relatively arid and salty habitats(*39*). Even many *Flaveria* species with different photosynthesis pathways also appear in the same area(*42*). For example, *Flaveria pringlei* (C_3) and *Flaveria kochiana* (C_4) grow adjacent to each other in the same place. *F.ramosissima* and their C_3 relatives appear in similar regions and habitat types, and there is no obvious climate or location difference indicating that the growth conditions of the intermediates are more severe (*42*). In a recent inspection of the site characteristics and ecological physiology, Sudderth *et al*. shows no distinct functional difference between C_3 species and C_3-C_4 species, which existed in a common area in south-central Mexico (*42, 48*). Indeed, from the perspective of the C_4 evolutionary model *Flaveria* genus, our evidence showed that stomatal traits are more clearly changed with the innovation of

photosynthetic pathway relative to previous research (*9*) (Fig 1, Fig 2). The significant difference between the different photosynthetic types but no significant difference in the same photosynthetic types also implies that other factors have little effects (Fig 1b,c, Fig 2a,c). Our data strengthened the previous understanding that the photosynthetic pathway associate with g_{smax} and the decrease in g_{smax} and *SD* in C_4 plants and generalized it in dicotyledon (*9*).

We provided a direct evidence for the evolution of stomatal traits in the current C_4 evolutionary model, and exhibited an example for the stomatal evolution along the road to C_4. Our data showed that the evolving of stomata along the evolutionary path to C_4 is gradual, not abrupt (Fig 1, Fig 2). We showed the time when stomatal traits changed, specifically, it initially changed in Type II, and dramatically changed at C_4-like (Fig 1, Fig 2). Previous studies have deduced that in C_4 grass, the decrease in *SD* might be due to the restriction of stomatal development by vein increasing (*9, 13*). However, there is no significant change in stomatal trait in Type I in *Flaveria* (Fig 1, Fig2), while the vein density at this time has already changed greatly as previous work shown, especially in *F. sonorensis* (*43*). Therefore, stomatal development in C_4 evolution likely not necessarily was constrained by the veins developing, might because of the different mechanism in dicots. This indicates that the decrease in *SD* may not be explained by veins alone. Throughout the evolution of C_4 photosynthesis, the evolutionary trend is always less stomata and larger stomata (Fig 2g). Negative correlation supplying an advantage that modulation in g_{smax} with the minimal change in epidermal area allocation to stomata might explain the opposite trend in *SD* and *SS*, as the previous studies have shown (*10, 52*). However, the declined stomatal index demonstrate that stomatal development has been impeded (Fig 2i), indicating that the epidermis allocated to stomata was reduced. Therefore, the negative correlation should not be sufficient to explain the opposite trend. Genetic studies have shown that *SS* and *SD* are related, indicated by transgenic experiments of genes related to stomatal development have proved that changes in SD can also cause changes in SS (*53, 82*). Therefore, the opposite trend could be caused by the changed expression of stomatal development related genes, which in accord with the changes in the

expression of *FSTOMAGEN* that we have observed(Fig 5 b,c,d). Previous studies have shown that the *SS* is related to the size of genome, and the genome has increased gradually with the C_4 evolution in *Flaveria* (*47, 83*). Another explanation for the larger stomata might be the contribution of genome size during C_4 evolution in *Flaveria* genus.

Water limitation might have been a primary driver for the evolution of C_4 photosynthesis (*5-7*). The *F. sonorensis*, *F. angustifolia*, in Type I intermediate *Flaveria* species, g_{smax} were still similar to those in two C_3 *Flaveria* species, i.e. *F. cronquistii*, *F. pringlei* and *F.robusta* (*2*) (Fig. 1b,c,d,e) (*84*). In contrast, the CO_2 concentration point of this Type I species was dramatically decreased (*85*) compared to their C_3 ancestors, as a result of an operating CO_2 concentrating mechanism of photorespiration CO_2 pump (C2 photosynthesis) (*86*). This suggests that during the evolution from C_3 to intermediate species, where the movement of GDC from mesophyll cell to bundle sheath cell occurred, the primary evolutionary driving force should be to elevate CO_2 levels around Rubisco, rather than H_2O saving (*87*). This coincides with the view of previous studies that improved carbon, not water, was the selection advantage for the early steps in the evolution of this genus C_4 (*2, 80*). After this step, reducing water loss might became crucial. The enhancement of photosynthetic capacity by C_2 photosynthesis can increase photosynthetic CO_2 uptake rate and evapotranspiration of leaf canopy, which can in principle create a higher water demand and increased the danger of embolism in the intermediate and later species, especially in the arid and semi-arid areas (*4*). Indeed, we found initial decline in g_{smax} occurred in Type II, especially in *F.ramosissima* (Fig 1b,c,d,e). It is worth noting that the decline in g_{smax} at this evolutionary stage could be significant for intercellular CO_2 concentration and supporting a high-strength photorespiratory CO_2 pump, which maximize the value of the high-strength photorespiratory CO_2 pump. Species with photorespiratory CO_2 pumps will actually have a greater advantage in environments that causing stomatal limitation (*84, 88*). The decrease in g_{smax} might indicates that the enhancement of photorespiration was promoted by stomatal limitation before this evolutionary stage, which will emphasize the advantage of

photorespiration CO_2 pump. Indeed, the photorespiratory CO_2 pump in *Flaveria* is established stepwise and the transcript and protein level of photorespiratory related genes was improved in Type II (*36, 38*). In a word, the decreased g_{smax} could strengthen the selection advantage of glycine localization to the bundle sheath cell. The gradual enhancement of the photorespiration CO_2 pump will make the problem of ammonia imbalance cannot be ignored, thus promoting the appearance of C_4 metabolism, as in the case in Type II (*33, 36*). Moreover, the emergence of C_4 photosynthesis could increase the photosynthetic capacity (*33, 36*) and allow the reduction of g_s to some extent. With further evolution of C_4 photosynthesis, we found that the dramatically decrease of g_{smax} occurred at C_4-like and subsequent C_4 (Fig 1b,c,d,e), that is, the process of the well-developed C_4 cycle. Due to the CA-PEPC enzyme and integrated C_4 cycle, although the partial pressure of CO_2 in the air space between leaf cells is largely reduced, the maximum photosynthetic rate can still be maintained. Therefore, the g_s indicated by the g_{smax} allowed be continually reduced. Our analysis provided an example for the relationship between the photosynthetic pathway and stomata at different stage of C_4 evolution, providing insights into the drivers on stomata and water carbon trade-off along the path to C_4. We do not deny the possible driving effect of water limitation in the C_4 evolution, but at least in the early stages in *Flaveria* genus, our evidence suggests that water limitation is not crucial and the optimization of water should be in the middle and late stages on the path to C_4 photosynthesis.

Since stomatal development is controlled by a molecular signaling network composed of many interacting components (*22*), in theory, Any genes controlling stomatal development could be potentially selected to alter stomatal pattern affecting g_{smax} during the emergence of C_4 photosynthesis (*11, 53*). In fact, changing the stomata pattern under different conditions does indeed choose different molecular pathways (*18, 89, 90*). Out of these different options, here we present results which indicate that a down-regulation of the expression of *FSTOMAGEN* (Fig 3c,e, Fig 5b,c,d), a *STOMAGEN*-like gene, has been selected as a molecular switch to alter stomatal pattern and further g_{smax} during the innovation of photosynthetic pathway in

Flaveria, which may be also the case in other C_4 lineages (Fig 6). Our evidences confirmed that the *FSTOMAGEN* strongly and positively regulates stomatal development by the synthetic FSTOMAGEN peptide applied in vitro and overexpression of *FSTOMAGEN* in Arabidopsis (Fig 4). Although other genes related to stomatal development also seem to be differentially expressed between C_3 and C_4, the degree of change is less than that of *FSTOMAGEN* (Fig 3c,d). *EPF1* and *TMM* are relatively more changed, but the direction is not consistent with the change in stomata. For example, *TMM* negatively regulates stomatal development, but its expression is lower in C_4, which is not consistent with the lower *SD* in C_4. The decrease in *TMM* and *EPF1* expression in C_4 may be due to the co-regulation of stomatal regulators, as previous work shows that overexpress *STOMAGEN* can increase the expression of other stomatal regulatory factors (*56*). The iWUE of *Flaveria* C_4 species relative to C_3 species increased significantly, partly contributed by the lower g_s (supplematry fig 1c,d). The magnitude of the decrease in g_s is matched by the magnitude of the decrease in g_{smax}, which indicates that g_{smax} contributes to the increased iWUE of C_4 species (Fig 1; Supplemary fig 1c,d). Therefore, the decrease in *FSTOMAGEN* expression could contribute to the increased iWUE in C_4 plants. In the C_4 engineering, it is inevitable to improve the water use of C_4 plants. Studies have shown that genes related to stomatal development do not only affect stomatal development, they can even affect photosynthetic apparatus and the development of photosynthetic tissues (*91*). Since the process of C_4 engineering is complicated, there is no guarantee that the stomatal engineering will not affect the engineering of other parts in C_4 syndrome. Since FSTOMAGEN was selected in the natural evolution of C_4 photosynthesis, at least the stomatal engineering would not cause unexpected damage to the C_4 engineering.

In conclusion, the features belong to C_4 syndrome have been found the suitable positions in the current C_4 evolution model. Although stomata have long been considered to be a member of the C_4 syndrome, their specific role along the path to C_4 is still unclear. In this study, with the C_4 evolutionary model genus *Flaveria*, we found the stomatal trait changed orderly with the innovation of photosynthetic pathway. The

changing process is gradual rather than abrupt on the path to C_4, and stomata always evolve towards less and larger. Our results showed the evolutionary direction and trajectory of stomata, providing insights into the evolutionary drivers, restriction and mechanism of stomata evolving along the road to C_4. The alter of stomatal traits mediated by *FSTOMAGEN* may contribute to the improvement of WUE in the later C_4 evolution. We provide an insight into carbon-water trade-offs in the current C_4 evolutionary model, and the molecular basis we found might help us improve WUE in C_4 engineering.

Reference

1. O. V. Sedelnikova, T. E. Hughes, J. A. Langdale, Understanding the Genetic Basis of C_4 Kranz Anatomy with a View to Engineering C_3 Crops. *Annu Rev Genet* **52**, 249-270 (2018).
2. P. J. Vogan, R. F. Sage, Water-use efficiency and nitrogen-use efficiency of C_3-C_4 intermediate species of Flaveria Juss. (Asteraceae). *Plant, cell & environment* **34**, 1415-1430 (2011).
3. S. H. H. Taylor, S. P. Rees, M Ripley, B. S. Woodward, F. I. Osborne, C. P., Ecophysiological traits in C_3 and C_4 grasses: a phylogenetically controlled screening experiment. *New Phytol* **185**, 780-791 (2010).
4. C. P. Osborne, L. Sack, Evolution of C_4 plants: a new hypothesis for an interaction of CO_2 and water relations mediated by plant hydraulics. *Philos Trans R Soc Lond B Biol Sci* **367**, 583-600 (2012).
5. H. Zhou, B. R. Helliker, M. Huber, A. Dicks, E. Akcay, C_4 photosynthesis and climate through the lens of optimality. *Proc Natl Acad Sci U S A* **115**, 12057-12062 (2018).
6. G. Reeves *et al.*, Natural Variation within a Species for Traits Underpinning C_4 Photosynthesis. *Plant physiology* **177**, 504-512 (2018).
7. B. P. Williams, I. G. Johnston, S. Covshoff, J. M. Hibberd, Phenotypic landscape inference reveals multiple evolutionary paths to C_4 photosynthesis. *Elife* **2**, e00961 (2013).
8. P. A. Christin, C. P. Osborne, The evolutionary ecology of C4 plants. *New Phytol* **204**, 765-781 (2014).
9. S. H. Taylor *et al.*, Photosynthetic pathway and ecological adaptation explain stomatal trait diversity amongst grasses. *New Phytol* **193**, 387-396 (2012).
10. P. J. Franks, P. L. Drake, D. J. Beerling, Plasticity in maximum stomatal conductance constrained by negative correlation between stomatal size and density: an analysis using Eucalyptus globulus. *Plant, cell & environment* **32**, 1737-1748 (2009).
11. T. Doheny-Adams, L. Hunt, P. J. Franks, D. J. Beerling, J. E. Gray, Genetic manipulation of stomatal density influences stomatal size, plant growth and tolerance to restricted water supply across a growth carbon dioxide gradient. *Philos Trans R Soc Lond B Biol Sci* **367**, 547-555 (2012).
12. W. M. Laetsch, The C4' syndrome: a structural analysis. *Ann. Rev. Plant Physiol.* **25**, 27-52 (1974).
13. D. A. Way, What lies between : the evolution of stomatal traits on the road to C4 photosynthesis. *New phytologist* **193**, 291-293 (2012).

696 14. T. W. Ocheltree, J. B. Nippert, P. V. Prasad, Changes in stomatal conductance along grass
697 blades reflect changes in leaf structure. *Plant, cell & environment* **35**, 1040-1049 (2012).
698 15. V. S. R. D. a. M. Santakumari, Stomatal characteristics of some dicotyledonous plants in
699 relation to the C_4 and C_3 pathways of photosynthesis. *Plant and cell physiology* **18**, 935-938
700 (1977).
701 16. E. J. Edwards, C. J. Still, Climate, phylogeny and the ecological distribution of C4 grasses. *Ecol*
702 *Lett* **11**, 266-276 (2008).
703 17. E. J. Edwards, C. J. Still, M. J. Donoghue, The relevance of phylogeny to studies of global
704 change. *Trends Ecol Evol* **22**, 243-249 (2007).
705 18. E. T. Hamanishi, B. R. Thomas, M. M. Campbell, Drought induces alterations in the stomatal
706 development program in Populus. *J Exp Bot* **63**, 4959-4971 (2012).
707 19. Q. Cai, C. Ji, Z. Yan, X. Jiang, J. Fang, Anatomical responses of leaf and stem of Arabidopsis
708 thaliana to nitrogen and phosphorus addition. *J Plant Res* **130**, 1035-1045 (2017).
709 20. Z. Xu, G. Zhou, Responses of leaf stomatal density to water status and its relationship with
710 photosynthesis in a grass. *J Exp Bot* **59**, 3317-3325 (2008).
711 21. N. Sekiya, K. Yano, Stomatal density of cowpea correlates with carbon isotope discrimination
712 in different phosphorus, water and CO2 environments. *New Phytol* **179**, 799-807 (2008).
713 22. N. Zoulias, E. L. Harrison, S. A. Casson, J. E. Gray, Molecular control of stomatal development.
714 *Biochem J* **475**, 441-454 (2018).
715 23. G. Lin *et al.*, A receptor-like protein acts as a specificity switch for the regulation of stomatal
716 development. *Genes Dev* **31**, 927-938 (2017).
717 24. E. D. Shpak, J. M. McAbee, L. J. Pillitteri, K. U. Torii, Stomatal patterning and differentiation by
718 synergistic interactions of receptor kinases. *Science* **309**, 290-293 (2005).
719 25. J. S. Lee *et al.*, Direct interaction of ligand-receptor pairs specifying stomatal patterning.
720 *Genes Dev* **26**, 126-136 (2012).
721 26. T. Shimada, S. S. Sugano, I. Hara-Nishimura, Positive and negative peptide signals control
722 stomatal density. *Cell Mol Life Sci* **68**, 2081-2088 (2011).
723 27. K. Hara, R. Kajita, K. U. Torii, D. C. Bergmann, T. Kakimoto, The secretory peptide gene EPF1
724 enforces the stomatal one-cell-spacing rule. *Genes Dev* **21**, 1720-1725 (2007).
725 28. L. Hunt, J. E. Gray, The signaling peptide EPF2 controls asymmetric cell divisions during
726 stomatal development. *Curr Biol* **19**, 864-869 (2009).
727 29. L. J. Pillitteri, K. U. Torii, Breaking the silence: three bHLH proteins direct cell-fate decisions
728 during stomatal development. *Bioessays* **29**, 861-870 (2007).
729 30. S. S. Sugano *et al.*, Stomagen positively regulates stomatal density in Arabidopsis. *Nature* **463**,
730 241-244 (2010).
731 31. T. Kondo *et al.*, Stomatal density is controlled by a mesophyll-derived signaling molecule.
732 *Plant Cell Physiol* **51**, 1-8 (2010).
733 32. L. Hunt, K. J. Bailey, J. E. Gray, The signalling peptide EPFL9 is a positive regulator of stomatal
734 development. *New Phytol* **186**, 609-614 (2010).
735 33. U. Schluter, A. P. Weber, The Road to C4 Photosynthesis: Evolution of a Complex Trait via
736 Intermediary States. *Plant Cell Physiol* **57**, 881-889 (2016).
737 34. R. Muhaidat, T. L. Sage, M. W. Frohlich, N. G. Dengler, R. F. Sage, Characterization of C(3)--C(4)
738 intermediate species in the genus Heliotropium L. (Boraginaceae): anatomy, ultrastructure
739 and enzyme activity. *Plant, cell & environment* **34**, 1723-1736 (2011).

740 35. D. Heckmann *et al.*, Predicting C4 photosynthesis evolution: modular, individually adaptive
741 steps on a Mount Fuji fitness landscape. *Cell* **153**, 1579-1588 (2013).
742 36. J. Mallmann *et al.*, The role of photorespiration during the evolution of C_4 photosynthesis in
743 the genus Flaveria. *Elife* **3**, e02478 (2014).
744 37. P. A. Christin, C. P. Osborne, R. F. Sage, M. Arakaki, E. J. Edwards, C(4) eudicots are not
745 younger than C(4) monocots. *J Exp Bot* **62**, 3171-3181 (2011).
746 38. S. Schulze *et al.*, Evolution of C4 photosynthesis in the genus flaveria: establishment of a
747 photorespiratory CO2 pump. *Plant Cell* **25**, 2522-2535 (2013).
748 39. A. M. Powell, Systematics of Flaveria (Flaveriinae--Asteraceae). *Annals of the Missouri*
749 *Botanical Garden* **65**, 590-636 (178).
750 40. A. D. MCKOWN, PHYLOGENY OF FLAVERIA (ASTERACEAE) AND INFERENCE OF C4
751 PHOTOSYNTHESIS EVOLUTION. *American Journal of Botany* **92**, 1911–1928 (2005).
752 41. E. A. Sudderth, R. M. Muhaidat, A. D. McKown, F. Kocacinar, R. F. Sage, Leaf anatomy, gas
753 exchange and photosynthetic enzyme activity in Flaveria kochiana. *Funct Plant Biol* **34**, 118-
754 129 (2007).
755 42. E. A. Sudderth, F. J. Espinosa-García, N. M. Holbrook, Geographic distributions and
756 physiological characteristics of co-existing Flaveria species in south-central Mexico. *Flora -*
757 *Morphology, Distribution, Functional Ecology of Plants* **204**, 89-98 (2009).
758 43. A. D. M. A. N. G. DENGLER, Key innovations in the evolution of Kranz anatomy and C4 vein
759 pattern in Flaveria (Asteraceae). *American Journal of Botany* **94**, 382–399 (2007).
760 44. U. Gowik, A. Bräutigam, K. L. Weber, A. P. M. Weber, P. Westhoff, Evolution of C_4
761 Photosynthesis in the Genus Flaveria: How Many and Which Genes Does It Take to Make C_4?
762 *The Plant Cell* **23**, 2087-2105 (2011).
763 45. N. Nakamura, M. Iwano, M. Havaux, A. Yokota, Y. N. Munekage, Promotion of cyclic electron
764 transport around photosystem I during the evolution of NADP-malic enzyme-type C4
765 photosynthesis in the genus Flaveria. *New Phytol* **199**, 832-842 (2013).
766 46. R. F. Sage, A portrait of the C4 photosynthetic family on the 50th anniversary of its discovery:
767 species number, evolutionary lineages, and Hall of Fame. *J Exp Bot* **68**, 4039-4056 (2017).
768 47. Y. Y. Taniguchi *et al.*, Dynamic changes of genome sizes and gradual gain of cell-specific
769 distribution of C4 enzymes during C4 evolution in genus Flaveria. *Plant Genome*, e20095
770 (2021).
771 48. F. Kocacinar, A. D. McKown, T. L. Sage, R. F. Sage, Photosynthetic pathway influences xylem
772 structure and function in Flaveria (Asteraceae). *Plant, cell & environment* **31**, 1363-1376
773 (2008).
774 49. M. Stata *et al.*, Mesophyll Chloroplast Investment in C3, C4 and C2 Species of the Genus
775 Flaveria. *Plant Cell Physiol* **57**, 904-918 (2016).
776 50. R. F. Sage, R. Khoshravesh, T. L. Sage, From proto-Kranz to C4 Kranz: building the bridge to C4
777 photosynthesis. *J Exp Bot* **65**, 3341-3356 (2014).
778 51. S. R. Christopher M. Hylton, Alison M. Smith, D. Alan Jones and Harold W. Woolhouse, Glycine
779 decarboxylase is confined to the bundle-sheath cells of leaves of C3-C4 intermediate species.
780 *planta* **175**, 452-459 (1988).
781 52. P. J. F. a. D. J. Beerling, Maximum leaf conductance driven by CO_2 effects on stomatal size and
782 density over geologic time. *PNAS* **106**, 10343–10347 (2009).

783 53. P. J. Franks, W. Doheny-Adams T, Z. J. Britton-Harper, J. E. Gray, Increasing water-use
784 efficiency directly through genetic manipulation of stomatal density. *New Phytol* **207**, 188-
785 195 (2015).
786 54. L. J. Pillitteri, K. U. Torii, Mechanisms of stomatal development. *Annu Rev Plant Biol* **63**, 591-
787 614 (2012).
788 55. S. Ohki, M. Takeuchi, M. Mori, The NMR structure of stomagen reveals the basis of stomatal
789 density regulation by plant peptide hormones. *Nat Commun* **2**, 512 (2011).
790 56. M. Hronkova *et al.*, Light-induced STOMAGEN-mediated stomatal development in
791 Arabidopsis leaves. *J Exp Bot* **66**, 4621-4630 (2015).
792 57. J. S. Lee *et al.*, Competitive binding of antagonistic peptides fine-tunes stomatal patterning.
793 *Nature* **522**, 439-443 (2015).
794 58. J. Lu *et al.*, Homologous genes of epidermal patterning factor regulate stomatal development
795 in rice. *J Plant Physiol* **234-235**, 18-27 (2019).
796 59. L. Xuxin, The Effects for Stomata Developmental on Arabidopsis by Overexpression of Rice
797 EPFL Family Genes. *Molecular Plant Breeding* **15**, 2042- 2047 (2017).
798 60. X. Yin *et al.*, CRISPR-Cas9 and CRISPR-Cpf1 mediated targeting of a stomatal developmental
799 gene EPFL9 in rice. *Plant Cell Rep* **36**, 745-757 (2017).
800 61. J. Y. Zhang, S. B. He, L. Li, H. Q. Yang, Auxin inhibits stomatal development through
801 MONOPTEROS repression of a mobile peptide gene STOMAGEN in mesophyll. *Proc Natl Acad*
802 *Sci U S A* **111**, E3015-3023 (2014).
803 62. M. J. Lyu *et al.*, RNA-Seq based phylogeny recapitulates previous phylogeny of the genus
804 Flaveria (Asteraceae) with some modifications. *BMC Evol Biol* **15**, 116 (2015).
805 63. M. A. Lyu *et al.*, The coordination of major events in C4 photosynthesis evolution in the genus
806 Flaveria. *Sci Rep* **11**, 15618 (2021).
807 64. K. Billakurthi *et al.*, Transcriptome dynamics in developing leaves from C_3 and C_4 Flaveria
808 species reveal determinants of Kranz anatomy. *bioRxiv*, (2018).
809 65. M. G. Grabherr *et al.*, Full-length transcriptome assembly from RNA-Seq data without a
810 reference genome. *Nat Biotechnol* **29**, 644-652 (2011).
811 66. B. Li, C. N. Dewey, RSEM: accurate transcript quantification from RNA-Seq data with or
812 without a reference genome. *BMC Bioinformatics* **12**, 323 (2011).
813 67. L. Wang *et al.*, Comparative analyses of C_4 and C_3 photosynthesis in developing leaves of
814 maize and rice. *Nat Biotechnol* **32**, 1158-1165 (2014).
815 68. X. Robert, P. Gouet, Deciphering key features in protein structures with the new ENDscript
816 server. *Nucleic Acids Res* **42**, W320-324 (2014).
817 69. D. R. F. Kyte J, A simple method for displaying the hydropathic character of a protein. *Journal*
818 *of Molecular Biology* **157**, 105-132 (1982).
819 70. S. Perveen *et al.*, Overexpression of maize transcription factor mEmBP-1 increases
820 photosynthesis, biomass, and yield in rice. *J Exp Bot* **71**, 4944-4957 (2020).
821 71. D. M. Emms, S. Kelly, OrthoFinder: solving fundamental biases in whole genome comparisons
822 dramatically improves orthogroup inference accuracy. *Genome Biol* **16**, 157 (2015).
823 72. R. C. Edgar, MUSCLE: multiple sequence alignment with high accuracy and high throughput.
824 *Nucleic Acids Res* **32**, 1792-1797 (2004).
825 73. A. Stamatakis, RAxML-VI-HPC: maximum likelihood-based phylogenetic analyses with
826 thousands of taxa and mixed models. *Bioinformatics* **22**, 2688-2690 (2006).

827 74. F. Ronquist *et al.*, MrBayes 3.2: efficient Bayesian phylogenetic inference and model choice
828 across a large model space. *Syst Biol* **61**, 539-542 (2012).
829 75. S. A. Shiryev, J. S. Papadopoulos, A. A. Schaffer, R. Agarwala, Improved BLAST searches using
830 longer words for protein seeding. *Bioinformatics* **23**, 2949-2951 (2007).
831 76. X. J. Min, G. Butler, R. Storms, A. Tsang, OrfPredictor: predicting protein-coding regions in
832 EST-derived sequences. *Nucleic Acids Res* **33**, W677-680 (2005).
833 77. A. L. Ming-Ju *et al.*, The Coordination and Jumps along C_4 Photosynthesis Evolution in the
834 Genus Flaveria. *bioRxiv*, 460287 (2018).
835 78. J. L. J. a. T. F. Ø. Claus Lindbjerg Andersen, Normalization of real-time quantitative reverse
836 transcription-PCR data a model-based variance estimation approach to identify genes suited
837 for normalization, applied to bladder and colon cancer data sets. *Cancer Res* **64**, 5245-5250
838 (2004).
839 79. D. P. K. Vandesompele J, Pattyn F, Poppe B, Van Roy N, De Paepe A, Speleman F., Accurate
840 normalization of real-time quantitative RT-PCR data by geometric averaging of multiple
841 internal control genes. *Genome Biology* **3**, research0034.0031–0034.0011 (2002).
842 80. D. A. Way, G. G. Katul, S. Manzoni, G. Vico, Increasing water use efficiency along the C_3 to C_4
843 evolutionary pathway: a stomatal optimization perspective. *J Exp Bot* **65**, 3683-3693 (2014).
844 81. A. V. a. D. C. Bergmann, Mechanisms of stomatal development: an evolutionary view.
845 *EvoDevo* **3**, (2012).
846 82. Y. Tanaka, S. S. Sugano, T. Shimada, I. Hara-Nishimura, Enhancement of leaf photosynthetic
847 capacity through increased stomatal density in Arabidopsis. *New Phytol* **198**, 757-764 (2013).
848 83. J. M. Beaulieu, I. J. Leitch, S. Patel, A. Pendharkar, C. A. Knight, Genome size is a strong
849 predictor of cell size and stomatal density in angiosperms. *New Phytol* **179**, 975-986 (2008).
850 84. P. J. Vogan, M. W. Frohlich, R. F. Sage, The functional significance of C_3-C_4 intermediate traits
851 in Heliotropium L. (Boraginaceae): gas exchange perspectives. *Plant, cell & environment* **30**,
852 1337-1345 (2007).
853 85. J. W. Maurice S. B. Ku, Ziyu Dai, Rick A. Scott, Chun Chu, and Gerald E. Edwards,
854 Photosynthetic and Photorespiratory Characteristics of Flaveria species. *Plant physiology* **96**,
855 518-528 (1991).
856 86. O. Keerberg, T. Parnik, H. Ivanova, B. Bassuner, H. Bauwe, C_2 photosynthesis generates about
857 3-fold elevated leaf CO_2 levels in the C_3-C_4 intermediate species Flaveria pubescens. *J Exp Bot*
858 **65**, 3649-3656 (2014).
859 87. R. F. Sage, T. L. Sage, F. Kocacinar, Photorespiration and the evolution of C_4 photosynthesis.
860 *Annu Rev Plant Biol* **63**, 19-47 (2012).
861 88. S. W, SCHUSTER* & R, K, MONSON An examination of the advantages of C3-C4intermediate
862 photosynthesis in warm environments. *Plant, Cell and Environment* **13**, 903-912 (1990).
863 89. C. B. Engineer *et al.*, Carbonic anhydrases, EPF2 and a novel protease mediate CO_2 control of
864 stomatal development. *Nature* **513**, 246-250 (2014).
865 90. Y. Tanaka, T. Nose, Y. Jikumaru, Y. Kamiya, ABA inhibits entry into stomatal-lineage
866 development in Arabidopsis leaves. *Plant J* **74**, 448-457 (2013).
867 91. G. J. Dow, J. A. Berry, D. C. Bergmann, Disruption of stomatal lineage signaling or
868 transcriptional regulators has differential effects on mesophyll development, but maintains
869 coordination of gas exchange. *New Phytol* **216**, 69-75 (2017).

92. M. Stata, T. L. Sage, R. F. Sage, Mind the gap: the evolutionary engagement of the C4 metabolic cycle in support of net carbon assimilation. *Curr Opin Plant Biol* **49**, 27-34 (2019).

Acknowledgements

The work was funded by Strategic Priority Research Program of the Chinese Academy of Sciences (grant number: XDB27020105) and the general program of National Science Foundation of China (31870214). We thank Prof. Rowan F. Sage (University of Toronto) for providing the Flaveria cuttings.

Author contributions

YYZ and XGZ designed the study. YYZ observed and measured the stomatal characteristic. YYZ carried out the molecular experiment and the treatment of synthetic peptides in vivo. FFM conducted the transgene experiment. GYC guided the treatment of peptides in vivo. Amy MJL analyzed the one kp RNA-seq data. YYZ and XGZ interpreted results and wrote the article.

Competing interests

The authors declare no competing financial interests.

Figure Legend

Fig 1: Maximum stomatal conductance (g_{smax}) of *Flaveria* species

a, Phylogenetic tree of Flaveria genus. **b**,**c**, The trend of g_{smax} on the abaxial surface in *Flaveria* species with different photosynthetic types from C_3 to C_4 grown outdoors (**b**) and in greenhouse (**c**). **d**,**e**, The difference in g_{smax} of the abaxial surface between species with different photosynthetic types in the *Flaveria* genus grown outdoors (**d**) and in greenhouse (**e**). **f**, Correlation of g_{smax} and g_s for *Flaveria* species with different photosynthetic types. Error bar indicates s.d. Different letters represent statistically significant differences (one-way ANOVA, Duncan's multiple range test (α = 0.05)). Pearson correlation coefficient and the significance were noted in each panel.

Fig 2: Stomatal density (*SD*) and its patterning.

a,**c**, The trend of *SD* of abaxial surface from C_3 to C_4 in *Flaveria* species grown outdoors (**a**) and in greenhouse (**c**). **b**,**d**, The difference in *SD* and guard cell length (l) of abaxial surface between species with different photosynthetic types in *Flaveria* genus grown outdoors (**b**) and in greenhouse (**d**). **e,** Correlation of g_{smax} and *SD* for different *Flaveria* species. Different color indicates different photosynthetic type. **f**, Correlation of g_{smax} and *l* for different *Flaveria* species. Different color indicates different photosynthetic type. **g**, Correlation of *l* and *SD* for different *Flaveria* species. Different color indicates different photosynthetic type. **h,** The photographs of stomatal patterning on abaxial surface in *rob*, *ram* and *bid*. The photographs from the left to right are for *rob*, *ram* and *bid* grown outdoors (top) and in greenhouse (bottom). **i**, Comparison of stomatal index (*SI*) between *rob*, *ram*, and *bid*. Different colours represent plants grown outdoors (blue) or in greenhouse (green). *SD*, (n=4, biologically independent replicates). *l*, (n=20, biologically independent replicates). *SI*, (n=3, biologically independent replicates). Error bar indicates s.d. Different letters represent statistically significant differences (one-way ANOVA, Duncan's multiple range test (α = 0.05)). Pearson correlation coefficient and the significance are noted in each panel.

Fig 3: Transcript abundance of stomatal developmental related genes between C_3 and C_4 *Flaveria* species.

a, A model of the signaling pathway for the stomatal development in Arabidopsis (*22*). A protodermal cell (PDC, white) becomes a meristemoid mother cell (MMC, orange), which divides asymmetrically into two daughter cells, with one being a meristemoid (M, red) and the other being a stomatal-lineage ground cell (SLGC). The M cell develops into a guard mother cell (GMC, yellow); the SLGC develops into a pavement cell (PC). The GMC conducts a symmetrical division to produce two equal-sized guard cells (GC, green). EPF1, EPF2 and STOMAGEN competitively bind to ER and TMM, which can deliver a signal to the YDA MAPK cascade. SPCH, MUTE and FAMA ultimately are inactivated through phosphorylation by the YDA MAPK cascade. **b**, Comparison of the expression of stomatal developmental related genes between juvenile and mature leaves. **c**, The foldchanges of stomatal development related genes for the C_3 and C_4 *Flaveria* species. Fold change means the ratio between the gene expression in a C_3 *Flaveria* specie and gene expression in a C_4 *Flaveria* specie under the same leaf development stage and growth condition as the C_3 *Flaveria* species. The expression data were from (*64*), (*36*), (*44*) and One Thousand Plants (1KP). **d,** The volcano plot for the expression of the stomatal development related genes between C_3 and C_4 *Flaveria* species. The expression data were from (*36*) and (*64*). **e**, Relative expression level determined by RT-qPCR and expression level determined by RNA-seq of *FSTO* (*FSTOMAGEN*) in *rob* and *bid*. (n=4, biologically independent replicates).

Fig 4: The Function of *FSTOMAGEN* in controlling the *SD*

a, Protein conservation analysis of the homologs of FSTOMAGEN in different species. The amino acid regions marked by green line and red line represent the signal peptide and the functional domain of FSTOMAGEN, respectively. Red letters represent conserved amino acids in most species, white letters with red backgrounds represent amino acid conserved across all species. **b**, The stomatal density for Arabidopsis leaves with FSTOMAGEN applied at different concentrations (n=8,

biologically independent replicates). **c**, The stomatal density for bid leaves with FSTOMAGEN applied at different concentrations (n=8, biologically independent replicates). **d**, The stomatal index (SI) for bid leaves with FSTOMAGEN applied at different concentrations (n=6, biologically independent replicates). Error bar indicates s.d. The asterisks represent statistically significant differences (P<0.05, t-test, two-tailed distribution, unpaired). **e**, The structure of recombinant genes used to transform Arabidopsis. AFSTO represents the recombination of the signal peptide of STOMAGEN from Arabidopsis and the functional domain of FSTOMAGEN from *F.robusta*. FSTO represents the intact STOMAGEN from *F.robusta*. **f**, **i**, The *SD* (**e**) and RNA-level (**h**) of the different transgenic Arabidopsis (FSTO) lines. **g**, **j**, The *SD* (**f**) and RNA-level (**i**) of the different transgenic Arabidopsis (AR) lines. **h**, Comparison of the transgenic FSTO lines and AR lines. **k**, Photographs of stomata in a leaf from Arabidopsis with FSTO and AFSTO over-expressed. Scar bar represents 20 um. Error bar indicates s.d. The n.s. represent statistically no significant differences (P>0.05, t-test, two-tailed distribution, unpaired).

Fig 5: Expression level of *FSTOMAGEN* at different stages of C_4 evolution.

a, Protein conservation analysis of the homologs of FSTOMAGEN between different species in the *Flaveria* genus. The amino acid regions marked by green line and red line represent the signal peptide and the functional domain of STOMAGEN, respectively. Red letters represent conserved amino acids in most species; white letters with red background represent amino acids conserved across all species. **b**, Expression levels of *FSTOMAGEN* at the different developmental stages of leaves in *rob* and *bid*. P denotes leaf primordia. Approximate leaf length for the different leaf stages was 0.3 cm (stage 1), 0.5 cm (stage 2), 1.5 cm (stage 3), 2 cm (stage 4), 3 cm (stage 5), 4 cm (stage 6), 6 cm (stage7) , 8 cm (stage 8) and 10 cm (stage 9). **c**, Comparison of relative expression levels of *FSTOMAGEN* between *rob*, *ram* and *bid*. (n=3, biologically independent replicates). **d,** Comparison of the expression levels of *FSTOMAGEN* between different species with different photosynthetic types in *Flaveria* genus. For RT-qPCR, C_3 species incude *pri* (n=5) and *rob* (n=13),

intermediates species includes *ang* (n=3), *ram* (n=5) and *vag* (n=3), C_4 species include *tri* (n=4), *aus* (n=3), *bid* (n=4) and *koc* (n=3). For RNA-seq, C_3 species include *pri* (n=4) and *rob* (n=4), intermediates species includes *ano* (n=4), *pub* (n=4), *chl* (n=4), *bro* (n=4), C_4 speices include *tri* (n=4) and *bid* (n=4). The relative expression indicates the measurements with RT-qPCR, and the others were measured with RNA-seq. The geometric means of *EF1a* and *ACT7* were used as the reference in the calculation of expression levels for other genes. Error bars indicate s.d. The asterisks represent statistically significant differences (P<0.05, t-test, two-tailed distribution, unpaired). Different letters represent statistically significant differences (one-way ANOVA, Duncan' s multiple range test (α = 0.05)).

Fig 6, Comparison of stomatal pattern and expression levels of stomatal development related genes in the C_4 lineages other than *Flaveria*

a, Stomatal characteristics for rice and maize. *SD*, (n=8, biologically independent replicates); *l*, (n=25, biologically independent replicates); *SI*, (n=3, biologically independent replicates); g_s, (n=8, biologically independent replicates). Error bar indicates s.d. The asterisks represent statistically significant differences (P<0.05, t-test, two-tailed distribution, unpaired). **b**, Photographs of stomatal pattern in rice and maize. Scale bars represent 50 μm. **c**, Comparison of transcript abundance of stomatal development related genes between rice and maize. The developmental stages of leaves were divided into 11 and 15 parts in rice and maize, respectively. R represents the leaves of rice, M represents the leaves of maize. **d**, Comparison of the expression levels of *STOMAGEN* homologs between rice and maize. There are one and two paralogs of *STOMAGEN* that is expressing in rice and maize, respectively. *OsSTO* represents the homologs of *STOMAGEN* in rice. *ZmSTO* represents the homologs of *STOMAGEN* in maize. **e**, The families and numbers of species with different photosynthetic type that we used to analyse. **f**, Comparison of the expression of C_4 related genes between species with different photosynthetic types. **g**, Comparison of the expression of *STOMAGEN* homologs between species with different

photosynthetic types. The asterisks represent statistically significant differences (P<0.05, t-test, two-tailed distribution, unpaired).

Fig 7：Schematic of the tactic change in the C_4 syndrome in the current C_4 model.

The position of the C_4 syndromes in the current C_4 model was shown. The arrows represent the gradual enhancement or weaken of each feature over the entire evolutionary gradient. Darker color means enhancement, lighter color means weaken. The yellow parts are related to the stomatal traits shown by our data. The rest is the previous research on the C_4 related features in *Flaveria genus (2, 36, 38, 43, 47-50, 92)*.

Legends for Supplemental Figures

Supplementary fig 1. a, Stomatal conductance (g_s) responses to net photosynthesis rate (*A*) under saturated light. The circles on the graph indicate larger g_s values in different photosynthetic types (Data from (*2, 80*)). **b**, The correlation of g_{smax} (abaxial + adaxial) and g_s. **c**, G_s, *A and iWUE* under saturated light between C_3 (rob, pri,cro) and C_4 (bid, tri and koc) *Flaveria* species. (Data from (*2, 80*)). **d**, G_s, *A and iWUE* under growth light between C_3 (rob) and C_4 (bid) *Flaveria* species (n=6, biologically independent replicates).

Supplementary fig 2. g_{smax} on the adaxial surface of leaves in *Flaveria*. **a**,**b**, The difference in g_{smax} in species with different photosynthetic types grown outdoors (**a**) or in greenhouse (**b**). **c**,**d**, The changes of g_{smax} on the adaxial leaf surface from C_3 to C_4 species in the *Flaveria* genus grown outdoors (**c**) and in greenhouse (**d**). (n=3, biologically independent replicates). **e**, Correlation of g_{smax} and g_s on the adaxial surface of leaves. Different letters represent statistically significant differences (one-way ANOVA, Duncan's multiple range test (α = 0.05)).

Supplementary fig 3. *SD* on the adaxial surface of leaves in *Flaveria*. **a**,**b**, The difference in *SD* in species with different photosynthetic types grown outdoors (**a**) or

in greenhouse (**b**). **c**,**d**, The changes of *SD* on the adaxial leaf surface from C_3 to C_4 species in the *Flaveria* genus grown outdoors (**c**) and in greenhouse (**d**). (n=3, biologically independent replicates). **e**, Correlation of g_{smax} and *SD* on the adaxial surface of leaves. **f**, Correlation of g_{smax} and *l* on the adaxial surface of leaves. **g**, Correlation of *l* and *SD* on the adaxial surface of leaves. Different letters represent statistically significant differences (one-way ANOVA, Duncan's multiple range test ($\alpha = 0.05$)).

Supplementary fig 4. *SD* in *rob* (C_3), *ram* (intermediate) and *bid* (C_4) grown from seeds. The *SD* on abaxial (ab) (n=5, biologically independent replicates) and adaxial (ad) (n=4, biologically independent replicates) surfaces were observed in *rob*, *ram* and *bid* grown in greenhouse. Different colours represent different photosynthetic types. Different letters represent statistically significant differences (one-way ANOVA, Duncan's multiple range test ($\alpha = 0.05$)).

Supplementary fig 5. Conservative analysis of amino acid sequences for EPF1 and EPF2. **a**. Comparison of amino acid sequences of homologs of EPF1 between different *Flaveria* species and Arabidopsis. **b**. Comparison of amino acid sequences of homologs of EPF2 between *Flaveria* species and Arabidopsis. White letters with red background represent amino acids conserved across all species. Red letters represent amino acids with similar biochemical property.

Supplementary fig 6. Hydrophobicity analysis of proteins. **a**, the protein of stomagen (left) and the protein of FSTOMAGEN (right). **b**, the protein of EPF1 (left) and the protein of FEPF1 (right). **c**, the protein of EPF2 (left) and the protein of FEPF2 (right).

Supplementary fig 7. Assessment of the stability of expression levels of reference genes. **a**,**b**, Comparison of the stability of expression levels of candidate reference genes in the *Flaveria* species by RNA-seq. **c**, Gel electrophoresis showing the specificity of the primers for candidate reference genes. From left to right, *ACT7*, *EF1a*, *J3*, *PNdO*, *CPN20*, *UBC9*, *GAPDH*, *F2N1.5*, *PSRP4*, *CACMS*, *HEME2*, and *UBQ11*. **d**, The coefficient of variations (CV) for the candidate reference genes. **e**, The expression stability for candidate reference genes calculated by Genorm. **f**, The expression stability for candidate reference genes calculated by Normfinder.

Supplementary fig 8. The expression levels of stomatal development related genes in *Flaveria* genus. Expression levels of stomatal development related genes in species with different photosynthetic types in the *Flaveria* genus by RNA-seq. Data from (*36*).

Supplementary fig 9. Relative expression levels of *FSTOMAGEN* and *SD* for *rob* (C_3) under different light conditions. (A) Relative expression levels for *FSTOMAGEN* under two different light conditions. (B) *SD* under two different light conditions. Natural light: the maximal photosynthetic photon flux density in the greenhouse was about 1300~1400 mmol m^{-2} s^{-1}. Light in the phytotron: 20~100 mmol m^{-2} s^{-1}. Reference gene used to calculate the expression level was *ACT7*. The asterisks represent statistically significant differences ($P<0.05$, t-test, two-tailed distribution, unpaired).

Supplementary fig 10. Relative expression levels of stomata development related genes determined with different reference genes and different primers. **a, b, c,** Quantification with different primers and the same *EF1a* reference gene. Relative expressions shown in **a and b** were determined using the same primer pairs while that in **c** used other primer pairs (See details of the primers used in Table S2). **d,** Relative expression levels determined with the gene *J3* used as the reference gene.

Supplementary fig 11. Transcript abundance of genes in the C_4 cycle and C_4 related transporters in *Flaveria* genus. Data was from the One Thousand Plants (1KP)(*62*, *63*). J represents juvenile leaves and M represents mature leaves. Different colours represent species with different photosynthetic types in the *Flaveria* genus. Red colour represents C_3 species, grey colour represents C_3-C_4 species, green colour represents C_4-like species, and blue colour represents C_4 species.

Supplementary fig 12. Alignment of the functional domain of *STOMAGEN* with transcripts from different *Flaveria* species by Blast. From the top to bottom, *F. robusta*, *F. pringlei*, *F. angustifolia*, *F. ramosissima*, *F. vaginata*, *F. australasica*, *F. bidentis*.

Supplementary fig 13. The expression level of *FSTOMAGEN* in different *Flaveria* species based on RT-qPCR (**a**) or RNA-seq (**b**). For RT-qPCR, *pri* (n=5), *rob* (n=13), *ang* (n=3), *ram* (n=5), *vag* (n=3), *tri* (n=4), *aus* (n=3), *bid* (n=4) and *koc* (n=3). For

RNA-seq, all species n=4. The relative expression indicates the measurements with RT-qPCR. RPKM indicates RNA-seq, data from (*36*). **c**, The relationship between *SD* and *FSTOMAGEN* expression in *Flaveria* species with different photosynthetic types.

Supplementary fig 14. Comparison of the expression level of *FEPF1* and *FEPF2* between *rob* and *bid Flaveria* species by RT-qPCR or RNA-seq. RNA-seq data from (*36*). *FEPF1* and *FEPF2* indicates the homologs of *EPF1* and *EPF2*.

Supplementary fig 15. The analysis for the *SD* of T2 generation of transgenic Arabidopsis (AFSTO and FSTO). **a**, Comparison of *SD* between WT and transgenic Arabidopsis AR, FSTO respectively. **b**, RNA level identification of transgenic Arabidospsis. Two independent lines was analyzed for each trangene event.

Supplementary fig 16. The increase of *SD* in cotyledon of *F. bidentis* (*bid*) with in vitro application of FSTOMAGEN. Photographs of the leaf surface in the untreated (control) and treated bid plants. scale bar, 20 mm.

Supplementary fig 17.a, Photographs of leaf surface taken with differential interference contrast microscope showing the increased stomata density in F. bidentis (bid) leaves with FSTOMAGEN applied. Scale bar represents 20 μm. b, Photographs of leaf surface taken with differential interference contrast microscope showing the increased stomata density in Arabidopsis leaves with FSTOMAGEN applied. Scale bar represents 20 μm.

Supplementary fig 18. Phylogenetic tree for FSTOMAGEN. blue represents dicotyledon, red represents monocotyledon and pink represents the *Flaveria* species. The gene tree of STOMAGEN based on bayesian-inference method.

Supplementary fig 19. a, Schematic of the progresssion of C_4 evolution in *Flaveria* genus. **b**, A stomatal graph taken with a light microscope showing stomatal parameters for *Flaveria* species which are needed to be measured to calculate the g_{smax}. The graph of stomata is *rob*. *l* (stomatal length), PL (pore length) and GCW (guard cell width). **c**, Correlation of the guard cell width and stomatal length (left), correlation of the stomatal length and pore length (right).

Supplementary fig 20. Photographs showing clustered stomata on a leaf for the transgenic Arabidopsis. Scar bar represents 10 um.

Supplementary table 1. Statistics for the mapping of the RNA-seq data of the juvenile and mature leaves in different species of the *Flaveria* genus.

Supplementary table 2. Primers used in this study

Supplementary table 3. The effect of genes related to stomatal development in Arabidopsis on stomatal phenotypes.

Supplementary table 4. The N50 of the mapping of the RNA-SEQ data taken from 1KP database for the juvenile and mature leaves

Supplementary table 5. The mapping rates of the mapping of the RNA-SEQ data taken from 1KP database for the juvenile and mature leaves.

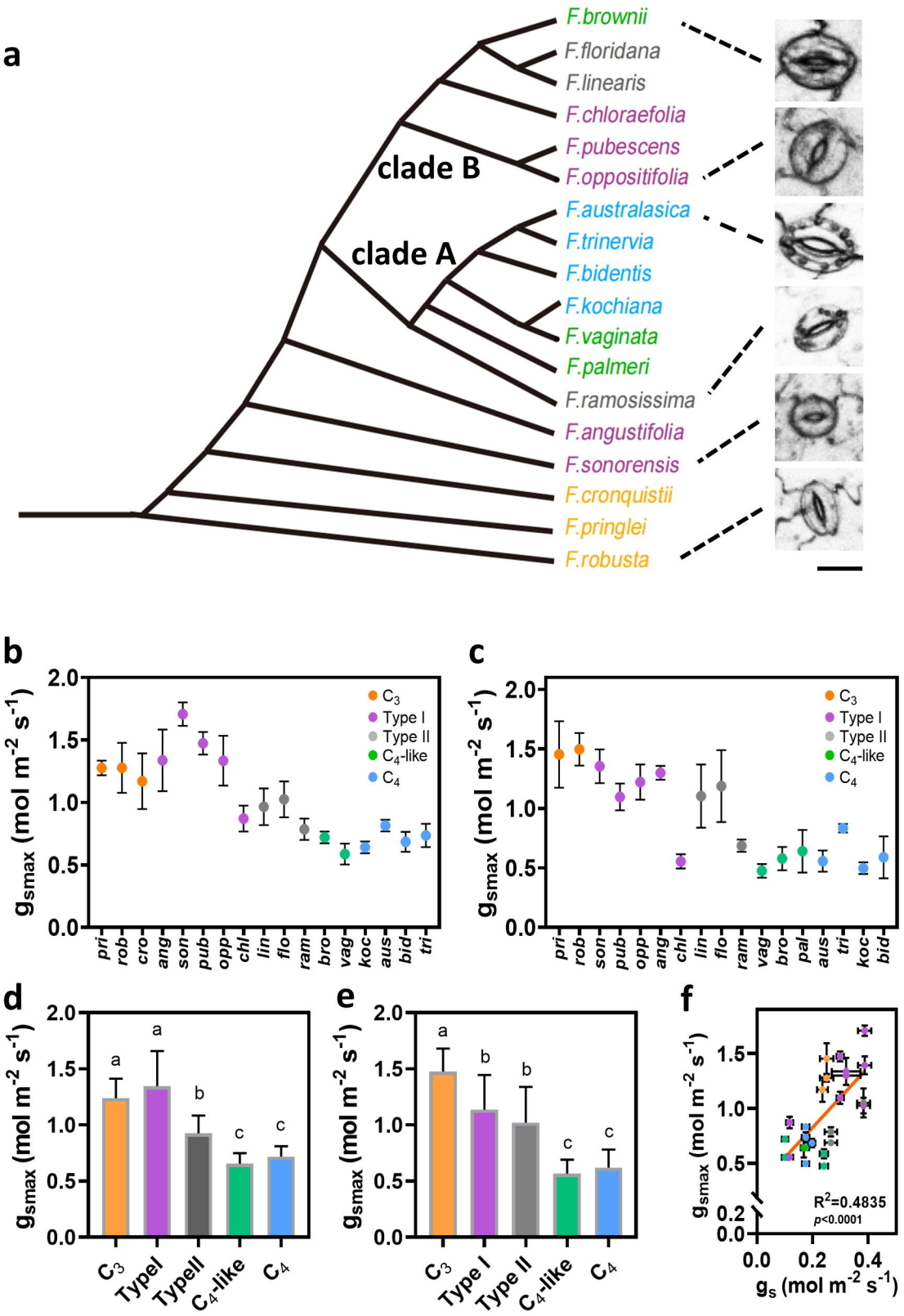
a
F.brownii
F.floridana
F.linearis
F.chloraefolia
F.pubescens
F.oppositifolia
F.australasica
F.trinervia
F.bidentis
F.kochiana
F.vaginata
F.palmeri
F.ramosissima
F.angustifolia
F.sonorensis
F.cronquistii
F.pringlei
F.robusta
clade B
clade A
b
c
d
e
f
g_{smax} (mol m^{-2} s^{-1})
C_3
Type I
Type II
C_4-like
C_4
pri rob cro ang son pub opp chl lin flo ram bro vag koc aus bid tri
pri rob son pub opp ang chl lin flo ram vag bro pal aus tri koc bid
R^2=0.4835
p<0.0001
g_s (mol m^{-2} s^{-1})

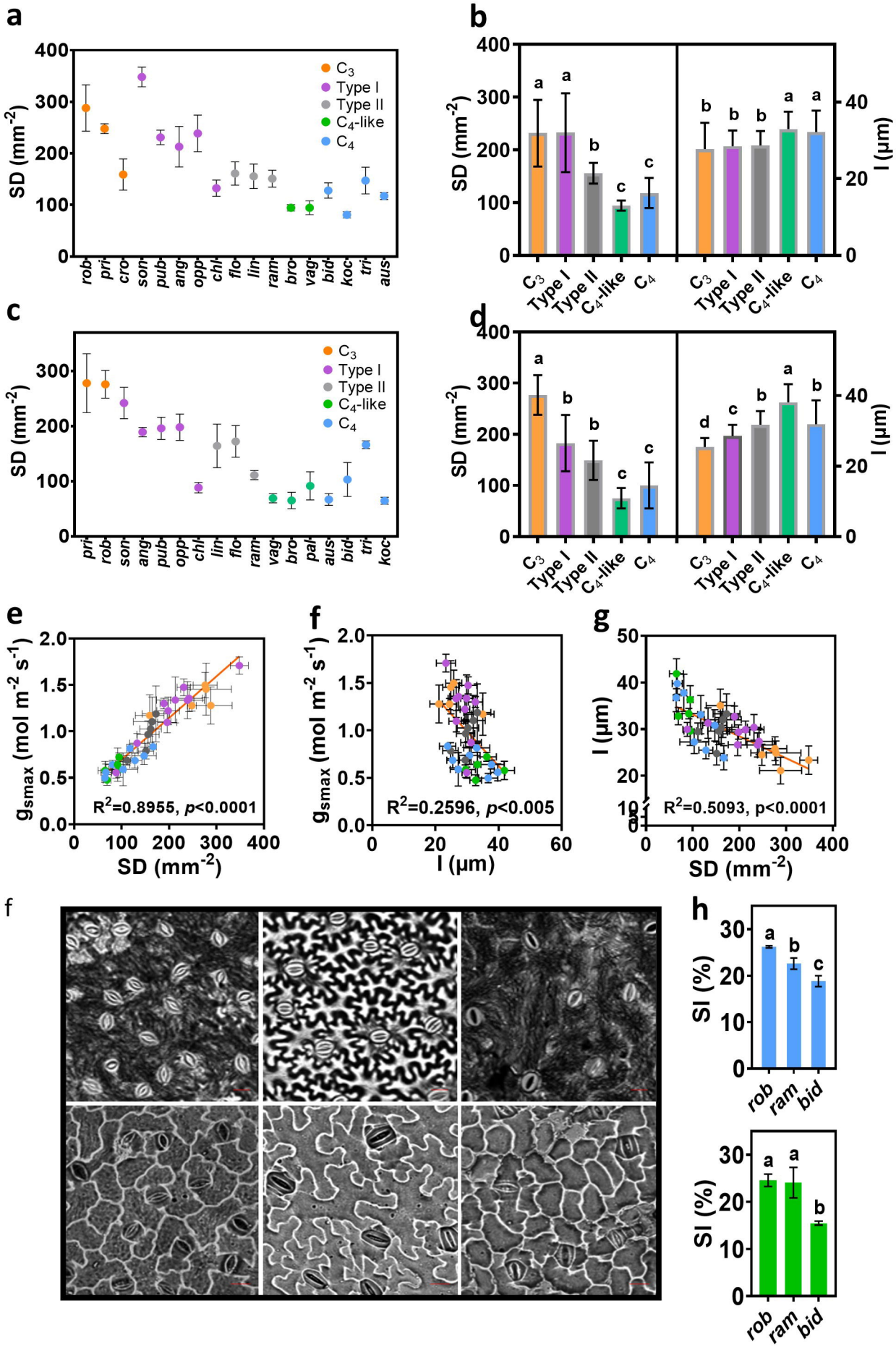
a
SD (mm-2)
C3
Type I
Type II
C4-like
C4
rob pri cro son pub ang opp chl flo lin ram bro vag bid koc tri aus
b
SD (mm-2)
I (µm)
C3 Type I Type II C4-like C4
c
SD (mm-2)
pri rob son ang pub opp chl lin flo ram vag bro pal aus bid tri koc
d
SD (mm-2)
I (µm)
e
gsmax (mol m-2 s-1)
R2=0.8955, p<0.0001
SD (mm-2)
f
gsmax (mol m-2 s-1)
R2=0.2596, p<0.005
I (µm)
g
I (µm)
R2=0.5093, p<0.0001
SD (mm-2)
f
h
SI (%)
rob ram bid
SI (%)
rob ram bid

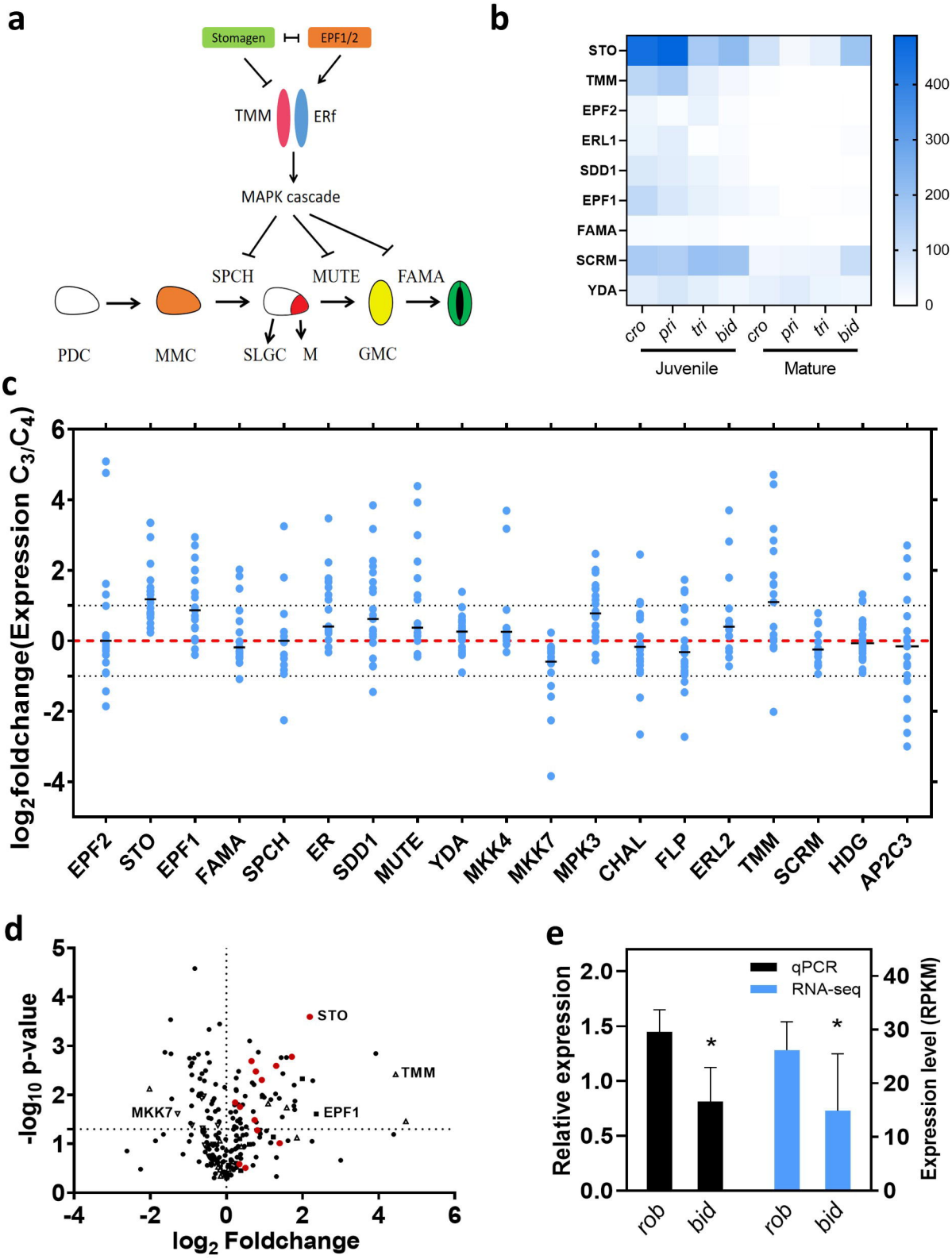
a
Stomagen
EPF1/2
TMM
ERf
MAPK cascade
SPCH
MUTE
FAMA
PDC
MMC
SLGC
M
GMC
b
STO
TMM
EPF2
ERL1
SDD1
EPF1
FAMA
SCRM
YDA
cro
pri
tri
bid
Juvenile
Mature
c
log2foldchange(Expression C3/C4)
EPF2
STO
EPF1
FAMA
SPCH
ER
SDD1
MUTE
YDA
MKK4
MKK7
MPK3
CHAL
FLP
ERL2
TMM
SCRM
HDG
AP2C3
d
-log10 p-value
log2 Foldchange
STO
TMM
MKK7
EPF1
e
Relative expression
Expression level (RPKM)
qPCR
RNA-seq
rob
bid

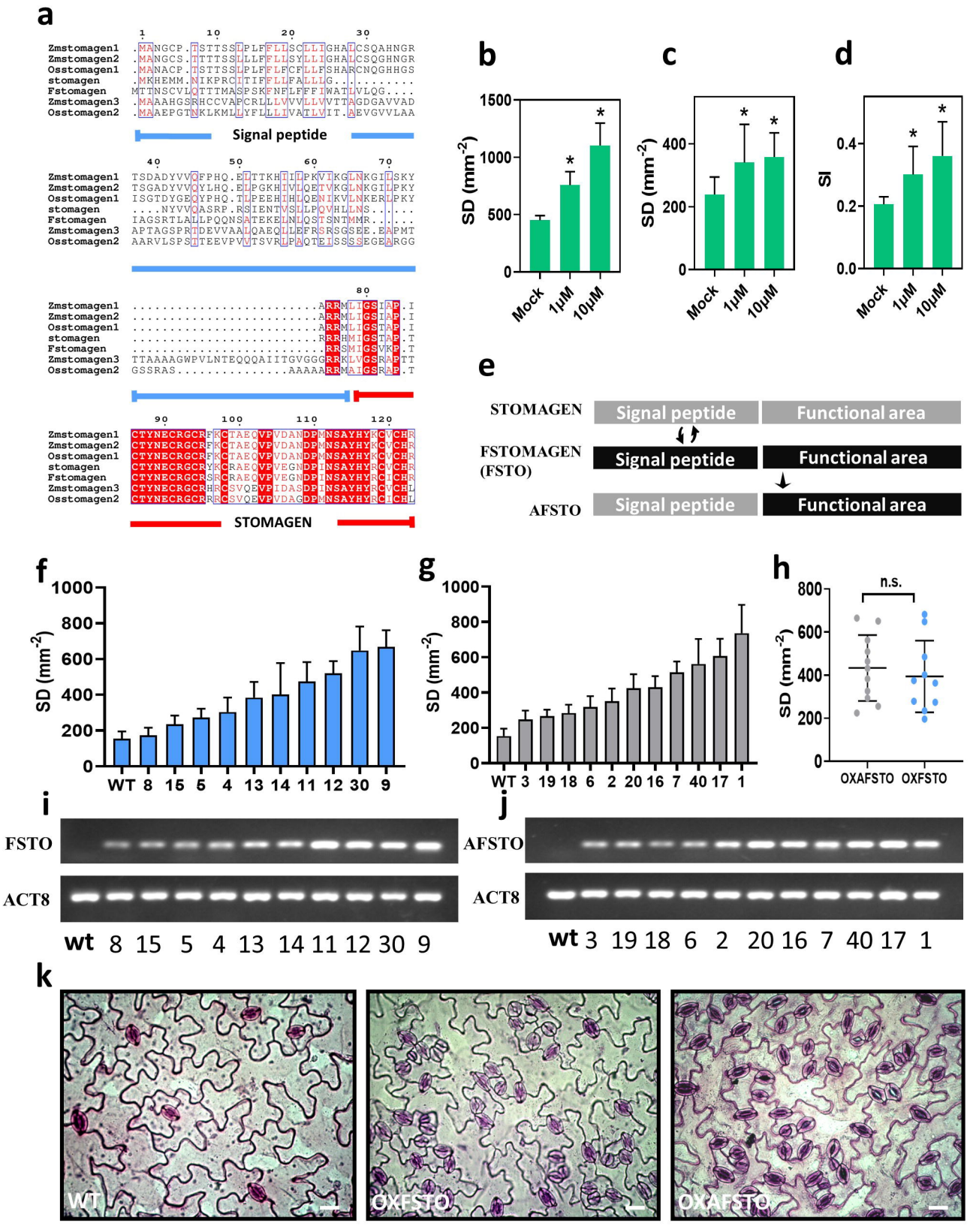
a
Zmstomagen1
Zmstomagen2
Osstomagen1
stomagen
Fstomagen
Zmstomagen3
Osstomagen2
Signal peptide
STOMAGEN
b
c
d
SD (mm-2)
SI
Mock
1μM
10μM
e
STOMAGEN
FSTOMAGEN (FSTO)
AFSTO
Signal peptide
Functional area
f
g
h
SD (mm-2)
WT 8 15 5 4 13 14 11 12 30 9
WT 3 19 18 6 2 20 16 7 40 17 1
n.s.
OXAFSTO
OXFSTO
i
j
FSTO
AFSTO
ACT8
wt 8 15 5 4 13 14 11 12 30 9
wt 3 19 18 6 2 20 16 7 40 17 1
k
WT
OXFSTO
OXAFSTO

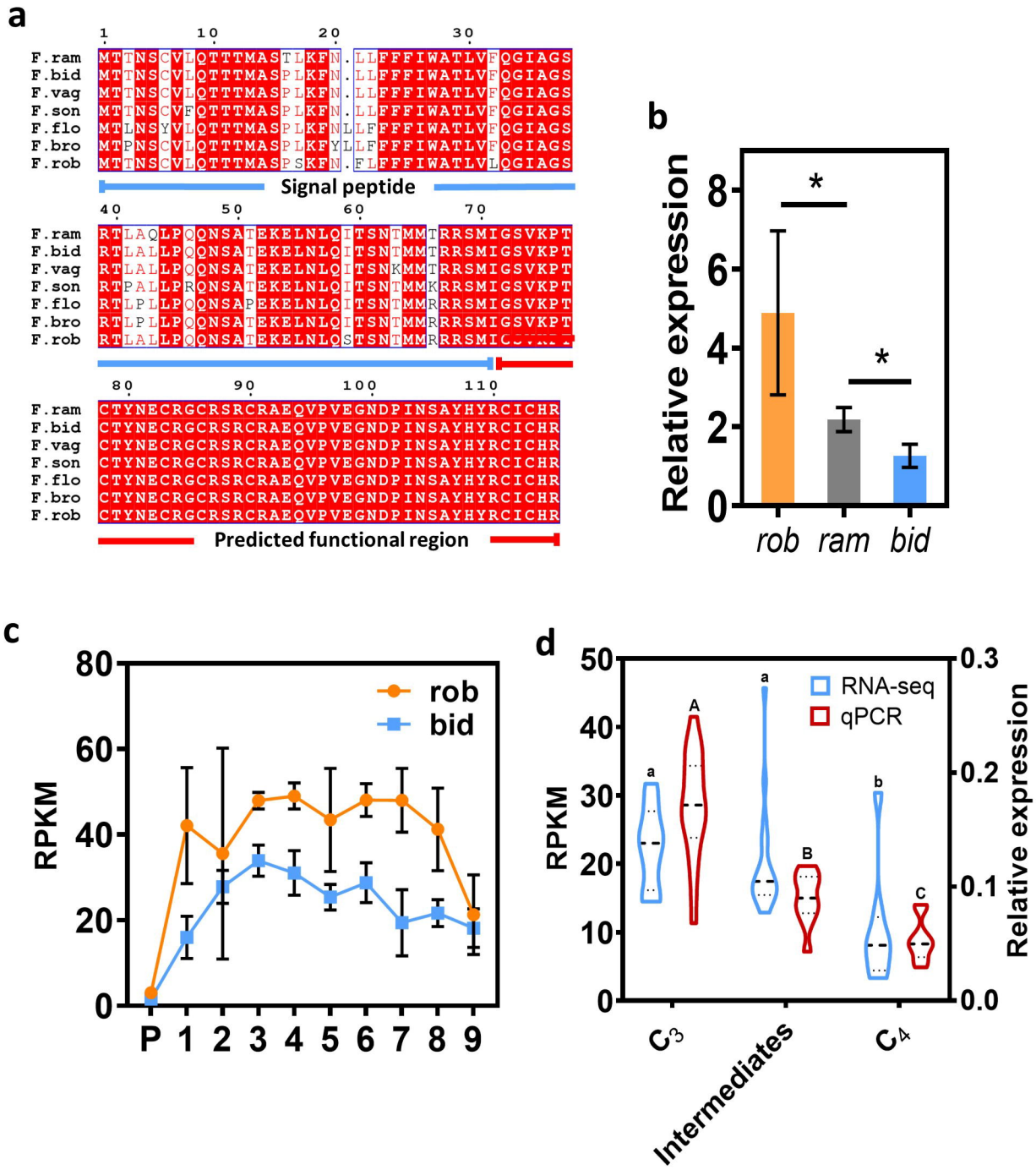
a
F.ram
F.bid
F.vag
F.son
F.flo
F.bro
F.rob
Signal peptide
Predicted functional region
b
Relative expression
rob
ram
bid
c
RPKM
rob
bid
P 1 2 3 4 5 6 7 8 9
d
RPKM
Relative expression
RNA-seq
qPCR
C3
Intermediates
C4

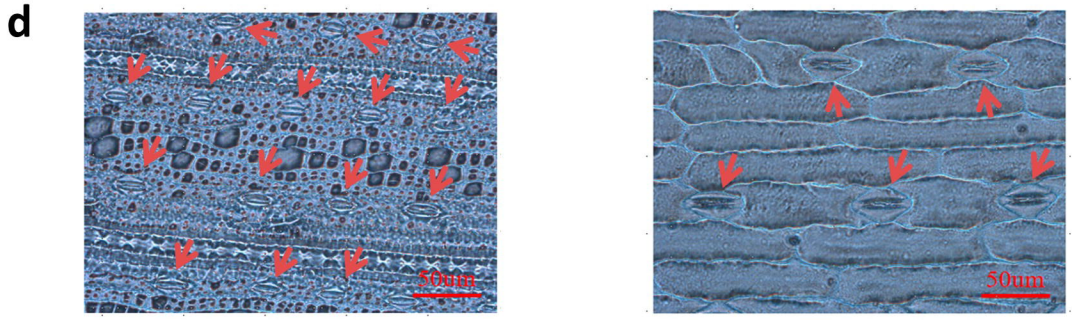

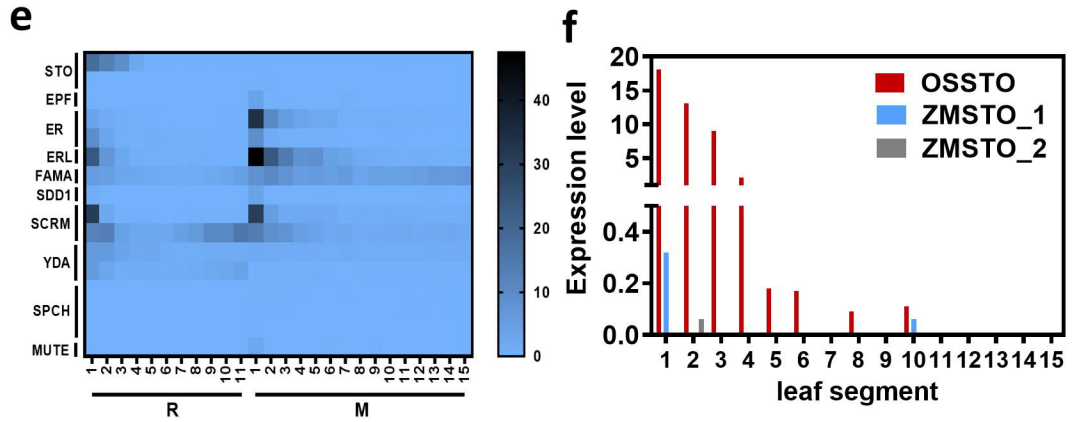

g

Family	Number
Poaceae	4
Aizoaceae	7
Amaranthacea	14
Chenopodiaceae	6
Molluginaceae	7
Nyctaginaceae	8
Portulacaceae	11
Zygophyllaceae	1
Euphorbiaceae	1
Cleomaceae	3
Boraginaceae	14
Scrophulariaceae	1
Total : C3(24); C4(41); C3-C4(12)	

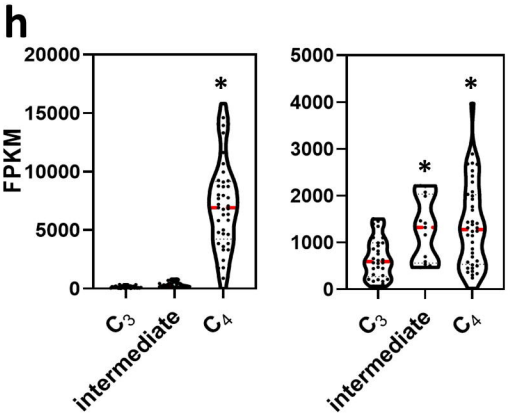

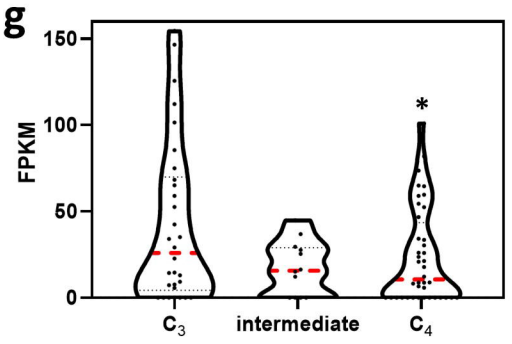

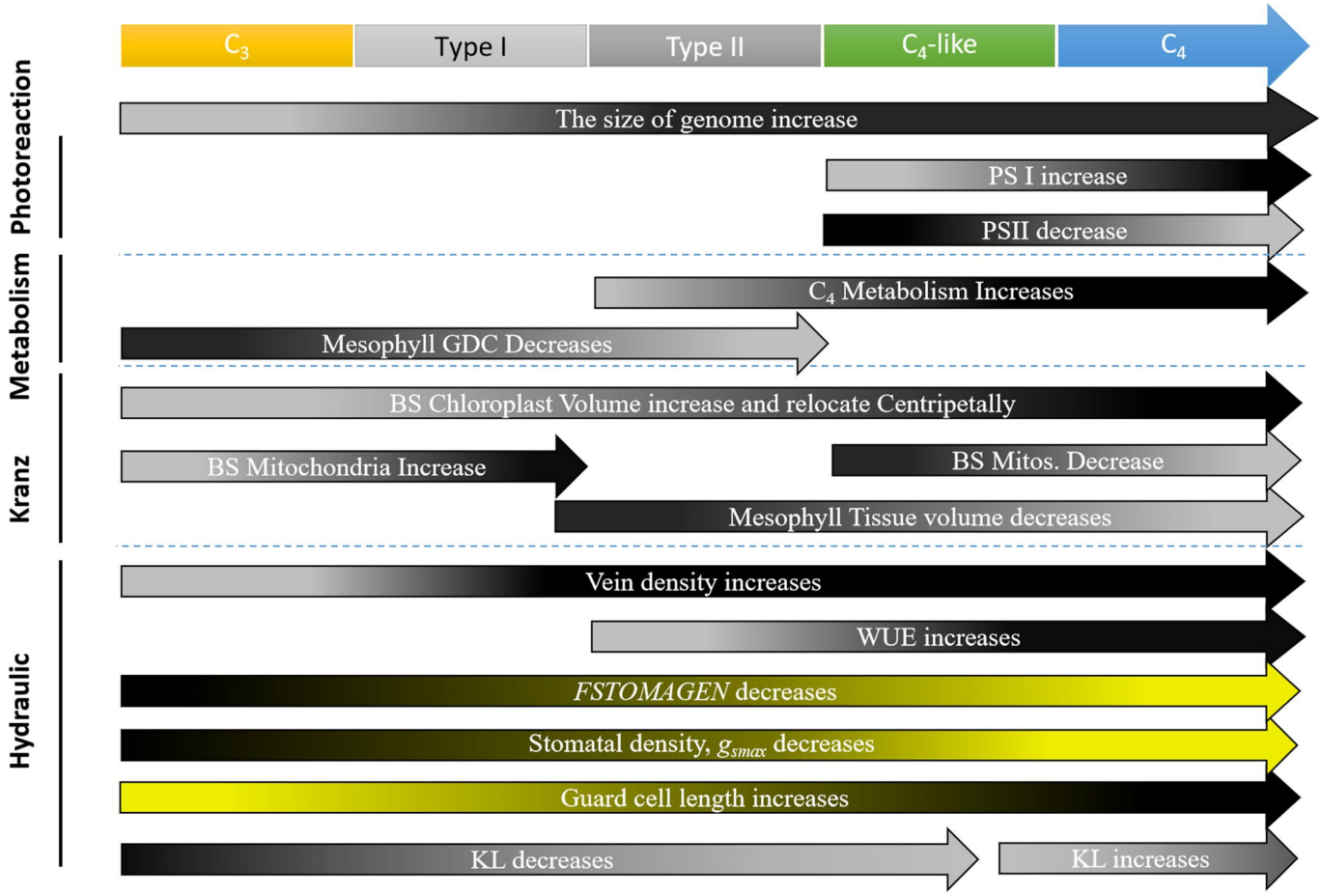
C3
Type I
Type II
C4-like
C4
Photoreaction
Metabolism
Kranz
Hydraulic
The size of genome increase
PS I increase
PSII decrease
C4 Metabolism Increases
Mesophyll GDC Decreases
BS Chloroplast Volume increase and relocate Centripetally
BS Mitochondria Increase
BS Mitos. Decrease
Mesophyll Tissue volume decreases
Vein density increases
WUE increases
FSTOMAGEN decreases
Stomatal density, gsmax decreases
Guard cell length increases
KL decreases
KL increases